Role of reservoir regulation and groundwater feedback in a simulated ground soil vegetation continuum: a long term regional scale analysis

Jianhui Wei, Ningpeng Dong, Benjamin Fersch, Joël Arnault, Sven Wagner, Patrick Laux, Zhenyu Zhang, Qianya Yang, Chuanguo Yang, Shasha Shang, Lu Gao, Zhongbo Yu, Harald Kunstmann

RESEARCH ARTICLE

WILEY

Role of reservoir regulation and groundwater feedback in a simulated ground-soil-vegetation continuum: A long-term regional scale analysis

Jianhui Wei[1] | Ningpeng Dong[2] | Benjamin Fersch[1] | Joël Arnault[1] | Sven Wagner[3] | Patrick Laux[1,4] | Zhenyu Zhang[1,4] | Qianya Yang[1,5,6] | Chuanguo Yang[5,6] | Shasha Shang[1,7] | Lu Gao[8,9] | Zhongbo Yu[5,6] | Harald Kunstmann[1,4]

[1]Institute of Meteorology and Climate Research (IMK-IFU), Karlsruhe Institute of Technology, Campus Alpin, Garmisch-Partenkirchen, Germany

[2]Department of Water Resources, China Institute of Water Resources and Hydropower Research, Beijing, China

[3]Gemeindewerke Mittenwald, Mittenwald, Germany

[4]Institute of Geography, University of Augsburg, Augsburg, Germany

[5]State Key Laboratory of Hydrology-Water Resources and Hydraulic Engineering, Hohai University, Nanjing, China

[6]College of Hydrology and Water Resources, Hohai University, Nanjing, China

[7]Key Laboratory of Western China's Environmental Systems (Ministry of Education), College of Earth and Environmental Sciences, Lanzhou University, Lanzhou, China

[8]Fujian Provincial Engineering Research Center for Monitoring and Assessing Terrestrial Disasters, Fujian Normal University, Fuzhou, China

[9]Institute of Geography, Fujian Normal University, Fuzhou, China

Correspondence
Jianhui Wei, Institute of Meteorology and Climate Research (IMK-IFU), Karlsruhe Institute of Technology, Campus Alpin, Garmisch-Partenkirchen, Germany.
Email: jianhui.wei@kit.edu

Ningpeng Dong, Department of Water Resources, China Institute of Water Resources and Hydropower Research, Beijing, China.
Email: dongnp@iwhr.com

Abstract

The regional terrestrial water cycle is strongly altered by human activities. Among them, reservoir regulation is a way to spatially and temporally allocate water resources in a basin for multi-purposes. However, it is still not sufficiently understood how reservoir regulation modifies the regional terrestrial- and subsequently, the atmospheric water cycle. To address this question, the representation of reservoir regulation into the terrestrial component of fully coupled regional Earth system models is required. In this study, an existing process-based reservoir network module is implemented into NOAH-HMS, that is, the terrestrial component of an atmospheric–hydrologic modelling system, namely, the WRF-HMS. It allows to quantitatively differentiate role of reservoir regulation and of groundwater feedback in a simulated ground-soil-vegetation continuum. Our study focuses on the Poyang Lake basin, where the largest freshwater lake of China and reservoirs of different sizes are located. As compared to streamflow observations, the newly extended NOAH-HMS slightly improves the streamflow and streamflow duration curves simulation for the Poyang Lake basin for the period 1979–1986. The inclusion of reservoir regulation leads to major changes in the simulated groundwater recharges and evaporation from reservoirs at local scale, but has minor effects on the simulated soil moisture and surface runoff at basin scale. The performed groundwater feedback sensitivity analysis shows that the strength of the groundwater feedback is not altered by the consideration of reservoir regulation. Furthermore, both reservoir regulation and groundwater feedback modify the partitioning of the simulated evapotranspiration, thus affecting the atmospheric water cycle in the Poyang Lake region. This finding motivates future research with our extended fully coupled atmospheric–hydrologic modelling system by the community.

1 | INTRODUCTION

The water cycle is strongly altered by human activities (Huntington, 2006; Laux et al., 2016; Oki & Kanae, 2006; Wada et al., 2017). Among them, reservoir regulation is one of the most prominent disturbances to the natural hydrologic system, since reservoirs are built worldwide as an effective measure to temporally, and in some cases spatially, redistribute water resources at the land surface for different purposes, for example, flood control (Zou et al., 2015), irrigation (Piao et al., 2010) and ecosystem maintenance (Suen & Eheart, 2006).

Parameterizing reservoir regulation in numerical models is a way to assess the anthropogenic impacts on the water cycle for both past and future expected periods (Pokhrel et al., 2016). Modelling studies showed that the inclusion of reservoir regulation alters the performance of hydrologic models and the simulated land surface processes (Gutenson et al., 2020; Jiang et al., 2020; Shin et al., 2019; Suen & Eheart, 2006; Yigzaw et al., 2019; Zajac et al., 2017; Zhao et al., 2016), such as improved estimates of streamflow (Veldkamp et al., 2018), increased evapotranspiration (Shah et al., 2019), and changed land surface water storage (Zhou et al., 2016). Furthermore, it offers opportunities for the assessment of impacts of reservoir regulation on water resources under projected climate change (Ehsani et al., 2017; Haddeland et al., 2014; Ngo et al., 2018; Wang, Lu, et al., 2017). Efforts in this direction have been made in several hydrologic models (Veldkamp et al., 2018; Wada et al., 2017), such as the LEAF-Hydro-Flood (LHF) model (Shin et al., 2019) and the Soil and Water Assessment Tools (SWAT) model (Liu et al., 2019). Applications of the extended hydrologic models have been made to case studies at basin scales (Adam et al., 2007; Lv et al., 2016; Ngo et al., 2018; Padiyedath Gopalan et al., 2021; Zhao et al., 2016), continental scales (Haddeland et al., 2006) and global scales (Biemans et al., 2011; Döll et al., 2009; Hanasaki et al., 2008a, 2008b).

Despite the importance of reservoir regulation in the water cycle, impact studies of reservoirs are primarily limited to the alteration of streamflow (Biemans et al., 2011; Dong et al., 2020; Gudmundsson et al., 2021; Jaramillo & Destouni, 2015; Zhao et al., 2021). Beyond the altered streamflow, reservoir regulation can also interact with other hydrological compartments, such as groundwater, soil, vegetations and their feedbacks, which is of high importance for the quantification and management of regional terrestrial water resources for different sectors (Barthel & Banzhaf, 2016; Condon & Maxwell, 2014; Somers et al., 2016), such as industry and agriculture (Li et al., 2018; Yao et al., 2018). By far, most of the existing hydrologic models with

reservoirs representation often have oversimplified groundwater processes and/or neglect the interaction between reservoir water and groundwater, for example, in SWAT (Liu et al., 2019). On the other hand, a number of hydrologic/hydraulic models with comparatively high complexity have been developed for the coupling of surface water and groundwater (Maxwell et al., 2014), like, for example, HydroGeoSphere (Brunner & Simmons, 2012). By using coupled models, feedback mechanisms between groundwater and surface water have been explored for semi-arid (Xie et al., 2018) or snow-dominant regions (Huntington & Niswonger, 2012). Studies showed that groundwater coupling results in considerable changes in the water fluxes at the land surface. However, such hydrologic/hydraulic models with sophisticated numerical algorithms for resolving three-dimensional groundwater processes often require detailed aquifer data and demand considerable computing resources, which may limit options for applications. Yet, relatively few studies in the context of surface water–groundwater interactions have shed light on the role of groundwater feedback in a reservoir-regulated ground-soil-vegetation continuum.

Climate models are coupled modelling frameworks that represent the physical processes at the Earth's surface for studying the past evolutions and future changes of the Earth (Claussen et al., 2002; Flato, 2011; Nazemi & Wheater, 2015a, 2015b; Pokhrel et al., 2016; Prinn, 2013). Recently, in the field of regional climate models (RCMs), fully coupled atmospheric–hydrologic models have been developed in order to account for the explicit description of surface and subsurface lateral water flows (Arnault et al., 2016; Arnault et al., 2018; Fersch et al., 2020; Powers et al., 2017; Wagner et al., 2016; Zhang et al., 2019). The inclusion of groundwater feedback into RCMs has been addressed as well in several recent studies (Maxwell et al., 2011; Shrestha et al., 2014; Wagner et al., 2016). Although the modification of the water cycle by intensive human activities is generally acknowledged, explicitly parameterizing human–water interactions into RCMs is still challenging (Nazemi & Wheater, 2015a, 2015b; Pokhrel et al., 2016). Only few efforts have been made to represent, for example, irrigation processes into RCMs (Guimberteau et al., 2012; Im & Eltahir, 2014; Qian et al., 2013; Sacks et al., 2009; Sorooshian et al., 2011). Results of these modelling studies show that irrigation can increase generation of shallow clouds and can lead to enhancement of rainfall in different climatic regions, such as the United States (Qian et al., 2013) and West Africa (Im & Eltahir, 2014). Recently, Keune et al. (2018) included a simplified human water use scenario into a coupled groundwater-to-atmosphere modelling system to study the human–water interactions for Europe. They stated that the local

scale human water use can have remote impacts via atmospheric processes. The modelling studies cited above either have neglected reservoir regulation and groundwater feedback processes or implicitly included the reservoir operation in the calibration of hydrologic models. However, recent studies suggest that such a practice can cause errors in hydrologic simulations under a changing environment, especially in highly regulated regions where reservoirs have a remarkable impact (Dang et al., 2020; Hoang et al., 2019).

The aim of this study is to implement a reservoir regulation module into the surface water–groundwater model interface of a fully coupled atmospheric–hydrologic modelling system and to quantitatively differentiate the regional *terrestrial* water cycle modified by reservoir regulation and by groundwater feedback. To this end, the reservoir regulation module of Dong, Yu, Yang, et al. (2019) has been incorporated into NOAH-HMS (Wagner et al., 2016), a combined modelling system consisting of the hydrological modelling system (HMS) (Yu et al., 2006) and the NOAH land surface model (LSM) (Chen & Dudhia, 2001). The NOAH-HMS model is chosen in our study because of its (1) distributed, process-based modelling approach with a sufficient level of complexity and (2) wide applicability. Specifically, NOAH-HMS has detailed descriptions of lateral movements of groundwater and explicit exchanges of water between saturated zone, unsaturated zone, lakes, wetlands or/and rivers (Fersch et al., 2013; Wagner et al., 2016; Yu et al., 2006). The two-dimensional groundwater module and the two-dimensional diffusive wave equation for resolving overland flow in NOAH-HMS allow to facilitate long-term, continental-scale applications with affordable computational costs. In addition, NOAH-HMS can be applied in a fully coupled mode, that is, coupled with the Weather Research and Forecast (WRF) model (Skamarock et al., 2008; Wagner et al., 2016), which has the potential for studying land-atmosphere interactions.

The regional focus of our study is on the Poyang Lake basin (27°N–30°N and 115°E–118°E). The choice of the Poyang Lake basin is motivated by the following two facts: (1) It has been reported that by 2007 about 9530 reservoirs and levees were found in the Poyang Lake basin and most of them were constructed before 1980s (Gu et al., 2017; Ye et al., 2013). Previous statistical studies revealed that human activities in the Poyang Lake basin including reservoir regulation have impacts on the basin-scale hydrological processes (Feng et al., 2012; Liu et al., 2013; Shankman et al., 2006; Zhang et al., 2016), such as mean annual streamflow (Ye et al., 2013; Zhang et al., 2011). (2) It has been recognized that the surface water–groundwater interaction in the floodplain of Poyang Lake has impacts on the spatial pattern and temporal variations of soil moisture (Xu et al., 2015), and vegetation dynamics (Zhang et al., 2017). More recent studies confirmed the importance of streamflow on modulating the groundwater levels and the role of groundwater levels on plant growth in the floodplain of Poyang Lake (Feng et al., 2020; Li et al., 2018). However, there exists a gap in knowledge about impacts of the reservoir-regulated rivers of the Poyang Lake basin on surface water–groundwater interactions on a basin scale.

Thus, the specific research questions addressed in this study are (1) how reservoir regulation in the Poyang Lake basin modifies the simulated regional terrestrial water cycle, (2) how groundwater feedback in the basin modifies the reservoir-regulated regional terrestrial water cycle and (3) to what extent the role of reservoir regulation and of groundwater feedback differ in a simulated ground-soil-vegetation continuum.

2 | MODELS AND METHODOLOGY

2.1 | The coupled surface water–groundwater model: NOAH-HMS

The two-way coupled surface water–groundwater model NOAH-HMS (Wagner et al., 2016; Yuan et al., 2009) is enhanced and employed for our reservoir regulation and groundwater feedback modelling study. NOAH-HMS consists of two components: the NOAH LSM model (Chen & Dudhia, 2001) is a spatially distributed LSM, accounting for vertical thermo-dynamical and hydrological processes at the land surface and in the soil, and the HMS model (Yu et al., 2006) is a spatially distributed hydrologic model, accounting for lateral hydrological processes at the land surface, in the soil, and within the saturated zone, using the 2-D diffusive wave equation, the equilibrium-state Richards equation, and the 2-D Boussinesq equation, respectively. It is noted that HMS here refers to a physically, raster-grid based model originally developed from BSHM (Yu & Schwartz, 1998), a basin-scale hydrologic model different from the HEC-HMS model developed by the United States Army Corps of Engineers.

The coupling strategy between two models is that NOAH is driven by meteorological forcing and provides runoff, evaporation and recharge to HMS. HMS routes overland-, subsurface- and streamflows, which alters soil moisture distribution and thereby impacts energy and water fluxes in NOAH. Details regarding the description of the NOAH-HMS model and the coupling strategy are given in Yuan et al. (2009) and Wagner et al. (2016).

2.2 | The soil-water and groundwater coupling method

In this study, the fixed-head groundwater–unsaturated zone bidirectional coupling method (de Rooij, 2010; Fersch et al., 2013; Zeng & Decker, 2009) is employed in order to investigate the role of groundwater feedback in a reservoir regulated ground-soil-vegetation continuum. The concept of the fixed-head method coupling soil water and groundwater is to replace the free drainage lower boundary condition of NOAH with a prescribed hydraulic head lower boundary condition, which assumes an equilibrium soil moisture profile between the groundwater level and the bottom soil layer of NOAH and thereby enables upward capillary rise.

2.3 | The reservoir network module incorporated into NOAH-HMS

The reservoir network module of Dong, Yu, Yang, et al. (2019) is incorporated into the NOAH-HMS model. This module accounts not only for changes in water stored in reservoirs and regulation of streamflow for the purpose of flood control and water supply, but also multiple hydrological processes related to reservoir regulation, such as the additional water surface evaporation, reservoir water–groundwater interaction, the variation of reservoir area across grid cells, with details given as follows.

To depict the role of reservoirs for streamflow regulation, the module employs size-dependent generalized rules of reservoir operation, that is, different rules of operation for large-sized (with a total storage capacity higher than 100 million m^3), medium-sized (with a total storage capacity between 10 and 100 million m^3), and small-sized (with a total storage capacity below 10 million m^3) reservoirs. This is because reservoirs in the Poyang Lake basin are different in terms of functionality and data availability.

For the large-sized and medium-sized reservoirs, four rules of reservoir operation are parameterized as follows: (1) if the stored water in reservoirs V_r (m^3) is less than the designed dead volume of reservoirs V_d (m^3), the outflow released from reservoirs Q_r (m^3 s^{-1}) is set to zero; (2) if V_r is in the range between V_d and the designed conservation volume of reservoirs V_c (m^3), Q_r is set to an adjusted outflow according to human/environmental water demands collected from the local authorities; (3) if V_r is in the range between V_c and the designed maximum flood-controlling volume of reservoirs V_f (m^3), Q_r is calculated by considering the balance between human/environmental water demands, the flood severity, and the purpose of keeping downstream regions away from inundation; (4) if V_r is more than V_f (m^3), Q_r is determined mainly by the maximum outflow from reservoirs $Q_{r,max}$ (m^3 s^{-1}) for maintaining safety of reservoirs.

For the small-sized reservoirs, three rules of reservoir operation are considered. The first two rules for operating small-sized reservoirs are same as the first two rules for operating large- and medium-sized reservoirs. The third rule for operating small-sized reservoirs is that if V_r is more than V_c, Q_r is calculated by considering the balance between human/environmental water demands and safety of reservoirs. Details on the parameterization of reservoir operation are given in Dong, Yu, Yang, et al. (2019).

The reservoir network module was originally integrated into the hydrological module (HMS) of a coupled land surface-hydrologic model system, namely CLHMS, and has been intensively validated for the Poyang Lake basin (Dong et al., 2020; Dong, Yu, Gu, et al., 2019; Dong, Yu, Yang, et al., 2019). Since NOAH-HMS and CLHMS consist of the same hydrological module, it is therefore straightforward to adapt the source code of the reservoir network module for the NOAH-HMS model.

Besides incorporating the reservoir regulation into HMS, we extend NOAH to additionally account for the subgrid-scale evaporation flux E_r (m s^{-1}) from reservoir water. The calculation of the evapotranspiration flux ET (m s^{-1}) in NOAH is then adjusted as follows:

$$ET = E_r(A_r/A_m) + (E_d + E_t)(1 - A_r/A_m) \qquad (1)$$

where A_r (m^2) and A_m (m^2) denote the area of reservoirs in one model grid cell and the area of the model grid cell, respectively. E_d (m s^{-1}) and E_t (m s^{-1}) are the direct evaporation flux and the transpiration flux from the land surface, respectively. A detailed description on the calculation of E_d and E_t is given in Chen and Dudhia (2001) and Wei et al., (2015). E_r is determined by the potential evaporation PE (m s^{-1}) calculated by a Penman-based approach (Mahrt & Ek, 1984) and the area of reservoirs:

$$E_r = PE \times A_r \qquad (2)$$

For the calculation of the area of reservoirs, we use the area–volume relationship derived and validated in our previous study of Dong et al. (2020):

$$A_r = \sqrt[1.5]{V_r/a} \qquad (3)$$

where V_r (m^3) and a (–) are the volume of reservoirs and the fitted shape coefficient, respectively. It is worth noting that the used area–volume relationship has been widely applied in numerous studies for understanding changes in water resources due to human actives (e.g., Wada et al., 2016). The area of reservoirs is calculated in HMS and then updated in NOAH after each iteration of HMS.

The water flux between the reservoir and the groundwater is considered and calculated in this study by using Darcy's law (Darcy, 1856) for saturated soil, that is, the head differences between the water level of reservoirs and that of groundwater multiplied by the saturated hydraulic conductivity for reservoirs. Due to the lack of local aquifer data, the saturated hydraulic conductivity for reservoirs is estimated by scaling the saturated hydraulic conductivity derived from the Chinese Geology dataset; the procedure of the estimation of saturated hydraulic conductivity for reservoirs is the following.

- Collect seepage of reservoirs documented by local authorities. It is found that the annual total seepage of reservoirs accounts for around 3% of the annual mean water storage.
- Estimate saturated hydraulic conductivity for documented reservoirs. The saturated hydraulic conductivity for documented reservoirs was estimated by trial and error – different values of saturated hydraulic conductivity were tested in the model for simulation of seepage, and the one gives seepage 3% of water storage was taken as a reasonable estimate of saturated hydraulic conductivity for each documented reservoir.
- Calculate the scaling factor between the estimated saturate hydraulic conductivity for documented reservoirs derived from the trial and error procedure and the saturated hydraulic conductivity from the Chinese Geology dataset.
- Estimate saturated hydraulic conductivity for remaining (undocumented) reservoirs. We assume that the scaling factor for the documented reservoirs is transferable and applicable to the remaining reservoirs in the basin. Then, the saturated hydraulic

conductivity for remaining reservoirs was estimated using the same scaling factor.

- Avoid unrealistic estimation of seepage from reservoirs. Additional threshold was set and applied in order to constrain the estimates of seepage from reservoirs being in a reasonable range of magnitude.

3 | THE EXPERIMENTAL DESIGN

3.1 | Study region

The Poyang Lake basin is located in the centre of Southeast China (Figure 1(b)) and covers in total an area of approximately 160 000 km^2 (Sun et al., 2012). The Poyang Lake basin encompasses five sub-basins of the Xiushui River (the sub-basin size: 3548 km^2), the Ganjiang River (80 948 km^2), the Fuhe River (15 811 km^2), the Xinjiang River (15 535 km^2) and the Raohe River (6374 km^2) shown in Figure 1 (b), and the five tributaries drain off into the largest freshwater lake in China, that is, Poyang Lake (an area of 3500 km^2 in a hydrologically normal year). The climate of the basin is characterized as humid subtropical, controlled by the East Asian monsoon (Ding & Chan, 2005). Therefore, the precipitation in the basin has distinct seasonality with a rainy season from April to June, and an unevenly spatial distribution with less than 600 mm year^{-1} in the North and more than 2000 mm year^{-1} in the South (Zhang et al., 2016).

Figure 2(a) shows the vegetation cover and land-use types for the Poyang Lake basin, which is based on the global 25-category data from the United States Geological Survey (USGS). Irrigated crop (land-use type 3) is the primary vegetation type in the basin with a fraction
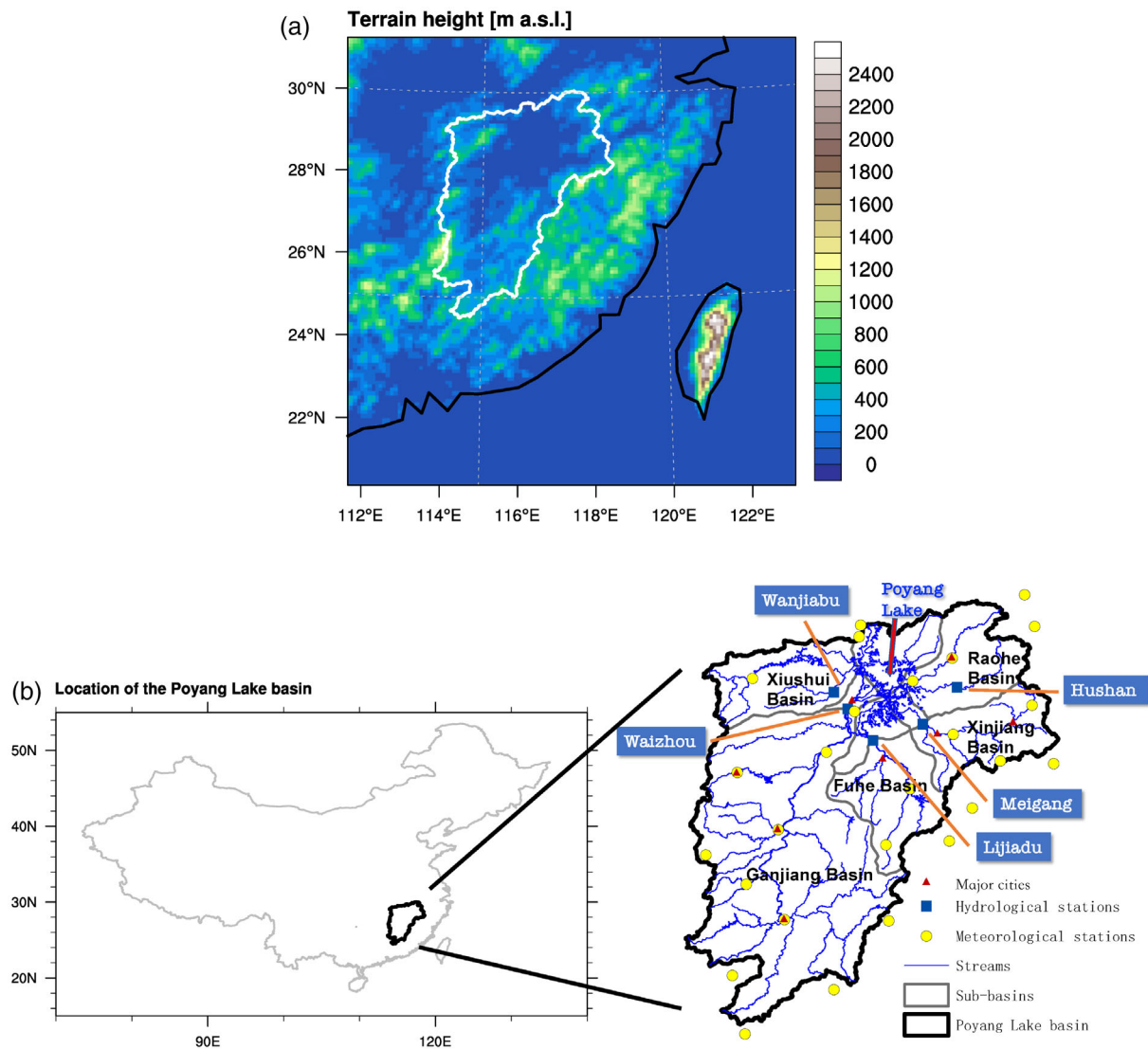
FIGURE 1 (a) The model domain setup and location of the Poyang Lake basin (white closed contour). The terrain height (m a.s.l.) of the simulation domain is shown in colour. (b) River network of the Poyang Lake basin and the lake area are shown in blue. The dark blue squares, the yellow circles, and the dark red triangles indicate the locations of the streamflow gauges, the meteorological stations, and the major cities in the basin, respectively

of 42%. Different types of forest dominate the remaining area of the basin. The terrain height of the Poyang Lake basin varies from higher than 2000 m a.s.l. in the South to lower than 50 m a.s.l. around the lake (Figure 2(b)).

3.2 | Model setup

For the setup of NOAH-HMS, we closely follow the model setup of Wagner et al. (2016). NOAH-HMS is configured over a 1240 km × 1240 km domain, which is centered over the Poyang Lake basin (see white frame in Figure 1(a)). The model has a horizontal resolution of 10 km × 10 km for a model grid of 124 × 124 in the longitude and latitude direction, respectively. The integration time steps of NOAH and HMS are 30 min and daily, respectively.

To drive the land-surface compartment NOAH model, the time-variant near-surface meteorological forcing is taken from daily observations at 26 meteorological stations (see yellow points in Figure 1(b)). The bilinear interpolation method is used to interpolate the station data to the 124 × 124 model grids (Figure 1(a)). To drive the hydrological compartment HMS model, the spatially distributed static hydro-geological information charactering the surface and subsurface conditions, such as hydraulic conductivity and river network, are derived from the Chinese Geology dataset and from the USGS 1 km digital elevation data set HYDRO1K. Regarding the detailed procedures for deriving the time-variant and static information for NOAH-HMS simulations, please refer to the study of Wagner et al. (2016).

For the reservoir network module, information about number of reservoirs, bathymetry, storage capacity and human water demand is acquired for the Poyang Lake basin from literature and the local authorities. In our modelling study, 1262 reservoirs (Figure 2(b)) are considered and parameterized because of the data availability of geographical and geometric information about reservoirs in the basin. Specifically, 24 large-sized (with a total storage capacity higher than 100 million m^3) and 234 medium-sized reservoirs (with a total storage capacity between 10 and 100 million m^3) were constructed before our simulation period, which is documented by the Yangtze River Water Resources Commission. The values of dead volume, flood-control volume, flood-design volume, maximum volume, maximum outflow of the 24 large-sized and 234 medium-sized reservoirs were collected from the Yangtze River Water Resources Commission as well, and then included in the static boundary condition of NOAH-HMS.

For 177 small-sized reservoirs (with a total storage capacity below 100 million m^3) information about location and maximum volume was collected from reports by the Jiangxi Provincial Water Resources Department. In addition, 827 small-sized reservoirs were identified by analysing the Landsat 8 remote sensing images of the Poyang Lake basin and the corresponding maximum volumes were estimated by employing the derived area–volume relationship. To close the gap between the total storage capacity of all small-sized reservoirs documented by the Jiangxi Provincial Water Resources Department and that of the 1004 small-sized reservoirs identified by
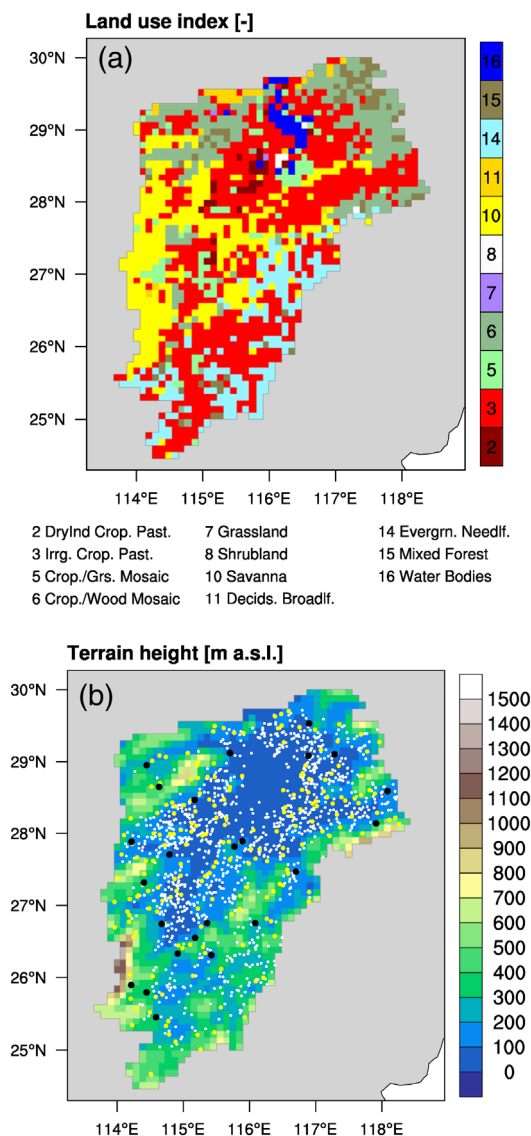

FIGURE 2 (a) Spatial distribution of the land-use types for the Poyang Lake basin with a horizontal resolution of 10 km × 10 km. The results are based on the global 25-category data from the United States geological survey (USGS). (b) Terrain height (m a.s.l.) of the Poyang Lake basin with a horizontal resolution of 10 km × 10 km. The individual black circles represent large-sized reservoirs with a storage capacity higher than 100 million m^3. The individual yellow circles represent medium-sized reservoirs with a storage capacity between 10 and 100 million m^3. The individual white circles represent small-sized reservoirs with a storage capacity below 10 million m^3

us, the differences in the total storage capacity were further allocated to the grid cells of croplands and their adjacent upstream grid cells using the method proposed by Dong, Yu, Yang, et al. (2019). The same procedure as the inclusion of the information about the large- and medium-sized reservoirs into NOAH-HMS is applied for processing the information on the small-sized reservoirs, but only for the maximum volume of reservoirs. In this study, the maximum volume of reservoirs are summed, if more than a single small-sized reservoir resides in a single 10 km × 10 km NOAH-HMS grid cell.

In this study, one reason why only the maximum volume was considered for the small-sized reservoirs is because the functionality of small-sized reservoirs in the Poyang Lake basin is different from that of the large- and medium-sized reservoirs: the small-sized reservoirs in the basin are designed mainly for irrigation practices and water supply at local scales for a regulation period within a year, whereas the large- and medium-sized reservoirs are designed mainly for flood-control and water resources management at the basin scale for multi-year regulation. The other reason is that, except for maximum volume, no other data was available for the small-sized reservoirs. Therefore, the flood-control function of small-sized reservoirs was neglected in the study.

3.3 | Simulation protocol

In this study, three simulations are conducted: (1) an original NOAH-HMS run with groundwater feedback, simulating the terrestrial water cycle without human alteration (ORG_GW); (2) a reservoir regulation-incorporated NOAH-HMS run with groundwater feedback, simulating the human-altered terrestrial water cycle (RES_GW); (3) a reservoir regulation incorporated NOAH-HMS run without soil water–groundwater two-way coupling, simulating human-altered terrestrial water cycle without groundwater feedback (RES_noGW). All three simulations are carried out for the period from 1977 to 1986. The first 2 years of the simulations are chosen as model spin-up time and are excluded from the analysis.

Regarding the calibration and validation of the original NOAH-HMS model, the previous study of Wagner et al. (2016) have manually calibrated (1978–1981) and validated (1982–1986) its most sensitive parameters in order to improve the reproduction of observed streamflow at five hydrological stations of the Poyang Lake basin (see blue squares in Figure 1(b)). Here, we set the values of the most sensitive four parameters, that is, the surface runoff-infiltration partitioning parameter (3.0), the bare soil evaporation exponent (1.0), the Manning's roughness coefficient (0.02 s $m^{-1/3}$), and the streambed hydraulic conductivity (10^{-5} s^{-1}), being same as the values taken by Wagner et al. (2016), for the whole period of our simulations.

For the reservoir regulation-incorporated NOAH-HMS, given that for most of the reservoirs in the Poyang Lake basin the operation data (inflow, outflow, storage, etc.) are unavailable for calibration of the reservoir network module, the values of the spatially distributed parameters in the reservoir network module, such as the water withdrawals from reservoir water for human use, the correction factor for adjusting the water withdrawals, and the maximum acceptable release rate of reservoirs for controlling floods, are estimated following the procedure of Dong et al. (2020).

3.4 | Reference data and evaluation strategy

For the evaluation of the simulations, station observations and gridded global datasets are used as reference data. For soil moisture,

surface runoff, and evapotranspiration, the product from the Climate Prediction Center (CPC) (Fan & van den Dool, 2004) is used. It provides gridded monthly global data at a spatial resolution of $0.5° \times 0.5°$. For streamflow, the daily observational records at the five hydrological stations (blue squares in Figure 1(b)) of the main tributaries in the Poyang Lake basin are used. To account for uncertainties in the evaluation of model performance, originating from single reference data, the Global Land Evaporation Amsterdam Methodology (GLEAM) product (Miralles et al., 2011) and a new data set of transpiration to evapotranspiration (Niu et al., 2020) (hereinafter referred to as Niu2020) are additionally employed for the purpose of further evaluation of the reservoir-regulation incorporated NOAH-HMS model performance. GLEAM provides the satellite-based 0.25° gridded monthly evapotranspiration at global scale for the 39-year period 1980–2018, which has been intensively used in evaluating regional climate simulations across the globe (e.g., Fersch & Kunstmann, 2014). Niu2020 provides the model-data fusion method-based, 0.05° gridded 8-day averaged transpiration to evapotranspiration ratio for China from 1981 to 2015, which has been validated against the in-situ observational annual transpiration to evapotranspiration ratios collected from the Chinese terrestrial ecosystem and against the available measurements collected from several field campaigns in China.

Four metrics are used for statically quantifying the skill of the simulations of streamflow Q at different temporal scales, namely, relative bias (RB, %), the Pearson's correlation coefficient (r, −), the Nash–Sutcliffe efficiency (NSE, −) (Nash & Sutcliffe, 1970) and the Kling–Gupta efficiency (KGE, −) (Gupta et al., 2009; Kling et al., 2012):

$$RB = \frac{\sum_{t=1}^{t=N}(S_t - O_t)}{\sum_{t=1}^{t=N} O_t} \times 100\% \tag{4}$$

$$r = \frac{\sum_{t=1}^{t=N}(S_t - \overline{S})(O_t - \overline{O})}{\sqrt{\sum_{t=1}^{t=N}(S_t - \overline{S})^2}\sqrt{\sum_{t=1}^{t=N}(O_t - \overline{O})^2}} \tag{5}$$

$$NSE = 1 - \frac{\sum_{t=1}^{t=N}(S_t - O_t)^2}{\sum_{t=1}^{t=N}(O_t - \overline{O})^2} \tag{6}$$

$$KGE = 1 - \sqrt{(r-1)^2 + \left(\frac{\sqrt{\frac{\sum_{t=1}^{t=N}(S_t - \overline{S})^2}{N}}/\overline{S}}{\sqrt{\frac{\sum_{t=1}^{t=N}(O_t - \overline{O})^2}{N}}/\overline{O}} - 1\right)^2 + \left(\frac{\overline{S}}{\overline{O}} - 1\right)^2} \tag{7}$$

where S_t (m^3 s^{-1}) and O_t (m^3 s^{-1}) denote the simulated and observed variable at the tth time step of evaluation, respectively. N is the total number of time step of evaluation. $\overline{S}$ (m^3 s^{-1}) and $\overline{O}$ (m^3 s^{-1}) denote mean of the simulated and observed variable, respectively. It is worth noting that KGE is additionally applied here in order to account for the uncertainty of the NSE-based evaluation results that may magnify errors in peak flows more than that in base flows (Knoben et al., 2019; Melsen et al., 2016).

4 | RESULTS

4.1 | Evaluation of streamflow simulated by NOAH-HMS

Figures S1 and 3 show the time series of streamflow observed (black lines) and simulated (blue lines) by the original NOAH-HMS model (ORG_GW) at the five gauges in the Poyang Lake basin for the investigation period from 1979 to 1986. Table 1 lists the model performance results using the evaluation metrics of RB, r, NSE and KGE.

At the daily scale, the observed streamflow at all five gauges are generally well reproduced by the ORG_GW simulation (Figure S1), with a mean r of 0.70 and a mean KGE (NSE) of 0.57 (0.45) (Table 1). The temporal variation of streamflow during the wet (March–June) and dry (July–February) months in ORG_GW matches the variation of the observation. Among the five gauges, the highest model performance in terms of r, NSE and KGE for reproducing daily observed streamflow is found at Waizhou, whereas the relatively lower model performance is found at Wanjiabu.

In comparison to the results at the daily scale, the values of the mean r and KGE (NSE) at the monthly scale increase to 0.94 and 0.78
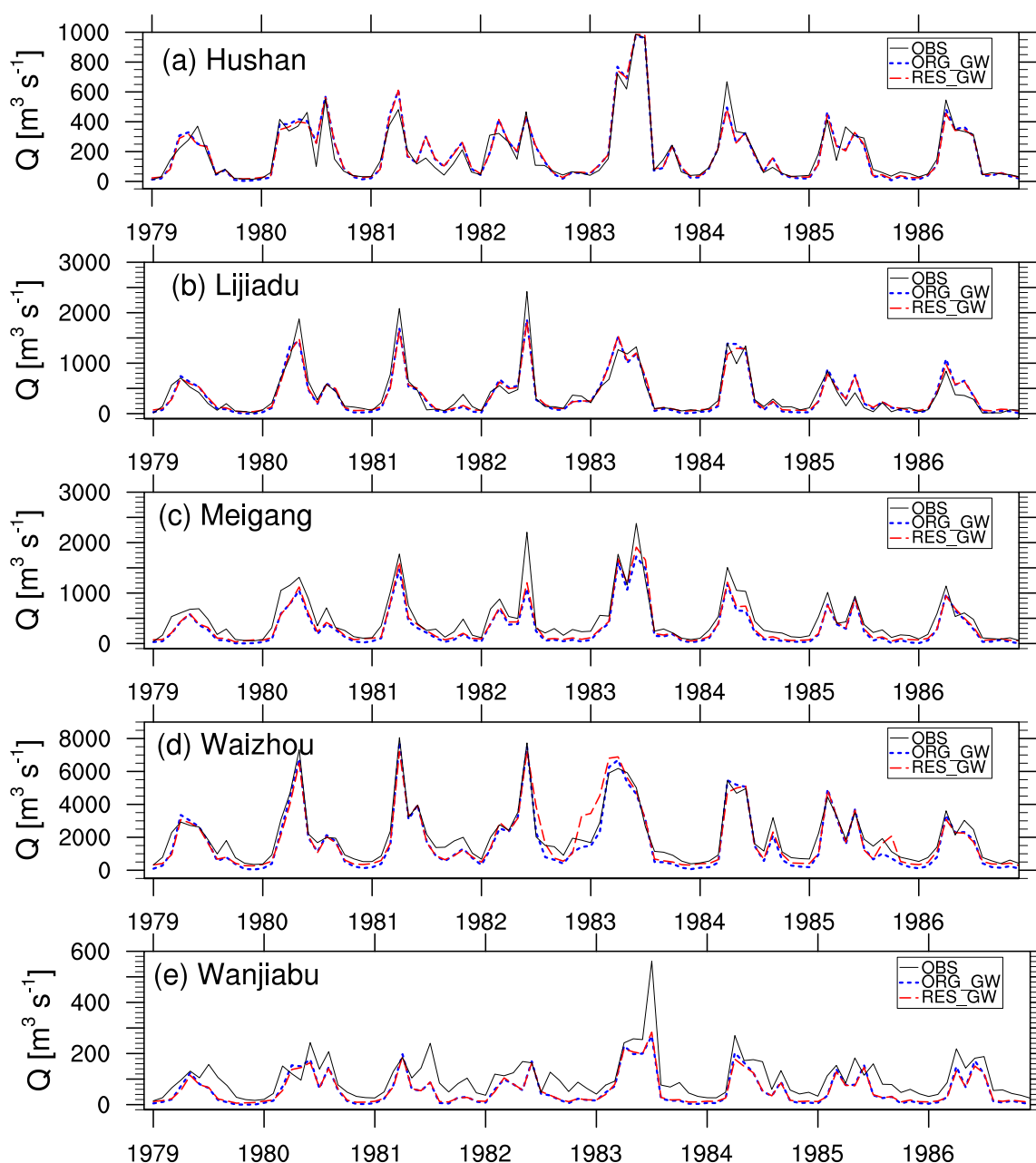

FIGURE 3   Monthly time series of streamflow Q (m^3 s^{-1}) from the observation (solid black line), the ORG_GW simulation (dashed blue line), and the RES_GW simulation (dashed red line) for the period from 1979 to 1986 at the five hydrological gauges of (a) Hushan, (b) Lijiadu, (c) Meigang, (d) Waizhou, and (e) Wanjiabu in the Poyang Lake basin

TABLE 1 Performance measures for daily and monthly streamflow from the ORG_GW (not in parentheses) and RES_GW simulations (in parentheses) against the observations at the five hydrological gauges in the Poyang Lake basin for the period from 1979 to 1986

	Daily				Monthly			
Gauge name	RB [%]	r [−]	NSE [−]	KGE [−]	RB [%]	r [−]	NSE [−]	KGE [−]
Hushan	1.45 (2.07)	0.62 (**0.63**)	0.32 (**0.35**)	0.60 (0.59)	1.28 (1.90)	0.96 (0.96)	0.92 (0.92)	0.95 (**0.96**)
Lijiadu	−4.51 (−**1.82**)	0.72 (**0.73**)	0.48 (**0.51**)	0.71 (0.69)	−4.82 (−**2.18**)	0.95 (**0.95**)	0.90 (**0.91**)	0.92 (0.89)
Meigang	−34.65 (−**26.12**)	0.75 (0.74)	0.50 (**0.52**)	0.47 (**0.52**)	−34.97 (−**26.50**)	0.95 (0.95)	0.76 (**0.82**)	0.61 (**0.70**)
Waizhou	−17.00 (−**9.23**)	0.88 (0.84)	0.74 (0.70)	0.79 (**0.81**)	−17.36 (−**9.60**)	0.98 (0.95)	0.91 (0.88)	0.81 (**0.88**)
Wanjiabu	−43.72 (−**43.15**)	0.55 (**0.57**)	0.21 (**0.24**)	0.27 (0.24)	−43.99 (−**43.46**)	0.85 (**0.87**)	0.41 (**0.42**)	0.49 (0.48)

Note: The performance measures that indicates improved streamflow simulations due to the incorporation of reservoir regulation are in bold.

(0.76), respectively (Figure 3 and Table 1). The relatively better model performance (NSE > 0.80, KGE > 0.85) for reproducing monthly observed streamflow is found at Waizhou, Lijiadu, Hushan. Although the model performance at Wanjiabu increases as well at the monthly scale, the absolute values of NSE and KGE are comparatively lower (NSE = 0.42, KGE = 0.48).

From the performance measures, we argue that our setup of the NOAH-HMS model has the ability to reproduce the observed daily and monthly streamflow at the five selected evaluation gauges in the study basin, which allows us to investigate the modification of reservoir regulation on the simulated terrestrial water cycle for the Poyang Lake basin and to explore the role of groundwater feedback in the simulated reservoir-regulated ground-soil-vegetation continuum.

4.2 | Role of reservoir regulation in a natural ground-soil-vegetation continuum

In this section, we investigate the role of reservoir regulation in the simulated terrestrial water cycle by comparing the reservoir regulation incorporated NOAH-HMS simulation (RES_GW) with the original NOAH-HMS simulation (ORG_GW) of Section 4.1. Both simulations allow groundwater feeding back to soil water using the fixed-head method of Section 2.2.

4.2.1 | Impact of reservoir regulation on streamflow simulation

Figures S1 and 3 (red lines) display the time series of the modelled streamflow in RES_GW, which shows that the daily and monthly variation of the observed streamflow is well captured by the reservoir regulation incorporated NOAH-HMS model. In comparison to ORG_GW, improved streamflow simulations are found in RES_GW (see bold numbers in Table 1). For example, at the daily and monthly scales, the values of RB decrease at 4 out of 5 gauges, with the highest decrease of around 8% at Meigang and Waizhou. The values of r in RES_GW either remain nearly identical or are slightly higher than these in ORG_GW. The reservoir regulation incorporation also yields a slightly improved model performance in terms of NSE and

KGE. However, among the five gauges, comparatively lower improved skill in RES_GW is achieved for simulating streamflow at Wanjiabu and Hushan. This may be attributed to the limited applicability of the large-scale NOAH-HMS to the streamflow simulation in relatively small sub-basins. Specifically, the drainage area of the Wanjiabu gauge and of the Hushan gauge is around 3500 and 6300 km^2, respectively, which is considered relatively small in view of a grid spacing of 10 km × 10 km. In addition, the terrain of drainage area of the Xiushui River (Wanjiabu) and the Hushan River (Hushan) are similarly characterized by steep topography and the number of reservoirs in the two sub-basins is lower than that in other three sub-basins (see Figure 2 (b)). Therefore, lower impact of reservoirs on streamflow regulation is found at Wanjiabu and Hushan. Moreover, the comparison of the streamflow duration curves derived from the RES_GW and ORG_GW simulations to that derived from the observations (Figure 4) suggests that the inclusion of reservoir regulation in the model results in generally improved reproductions of the distribution of observed streamflow amounts at daily and monthly scales, with slight reductions of the magnitude of simulated peak streamflow and large increases in simulated low streamflow. Overall, confirmed by the mostly improved statistical measures (Table 1) and improved streamflow return curves (Figure 4), the reservoir regulation incorporated NOAH-HMS model has the ability to slightly improve the streamflow simulation in the Poyang Lake basin in comparison to the original NOAH-HMS model, especially for the sub-basins where more reservoirs exist.

4.2.2 | Modification of simulated groundwater recharge, soil moisture, surface runoff, evapotranspiration and partitioned evapotranspiration

Figure 5(a) shows the spatial distribution of the simulated groundwater recharge GR from soils in RES_GW averaged for the period of 1979–1986, displaying that the values of GR in the western and eastern mountainous part of the basin are higher than these in the northern plain region around the lake. The basin-averaged GR has a strong monthly variation (Figure 5(b)), with higher values (>3 mm day^{-1}) in the rainy months (April–June) and lower values (<1 mm day^{-1}) in the relatively drier months (July–March).
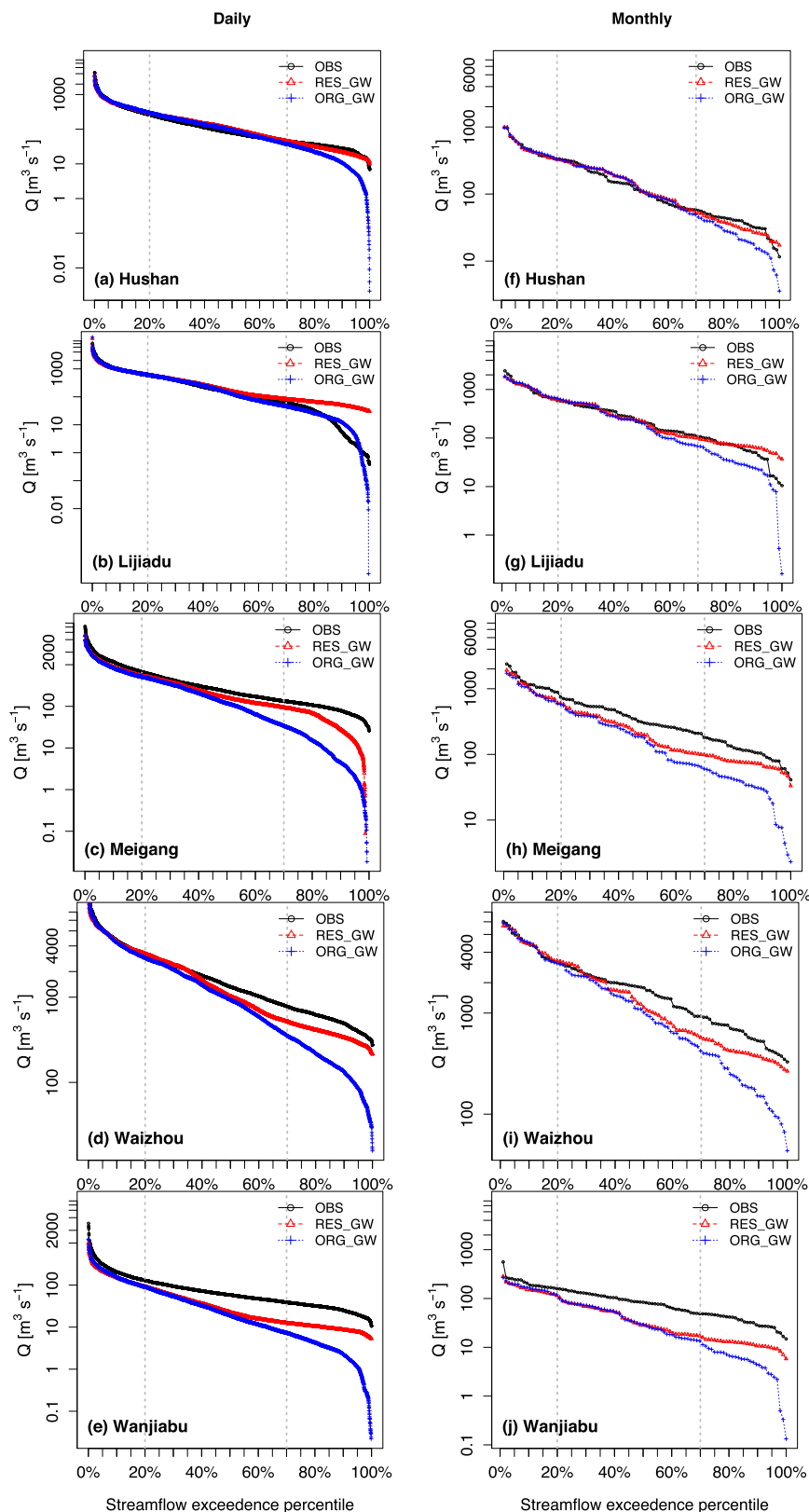
FIGURE 4 Daily (left column) and monthly (right column) streamflow duration curves (%) derived from the observation (black), the ORG_GW simulation (blue), and the RES_GW simulation (red) for the period 1979–1986 at the five hydrological gauges of (a, f) Hushan, (b, g) Lijiadu, (c, h) Meigang, (d, i) Waizhou, and (e, j) Wanjiabu

In comparison to ORG_GW, the incorporation of reservoir regulation generally results in a decreased *GR* from soils in RES_GW. The decrease in *GR* is more pronounced in the area where more water is stored in the reservoirs (Figure 5(c)) and during the rainy months (Figure 5(d)). This is because of that reservoir incorporation not only enhances the interaction from river water to groundwater, but also simulates a higher groundwater level in relation with the reservoir seepage. As a result, the hydraulic gradient between the soil water in
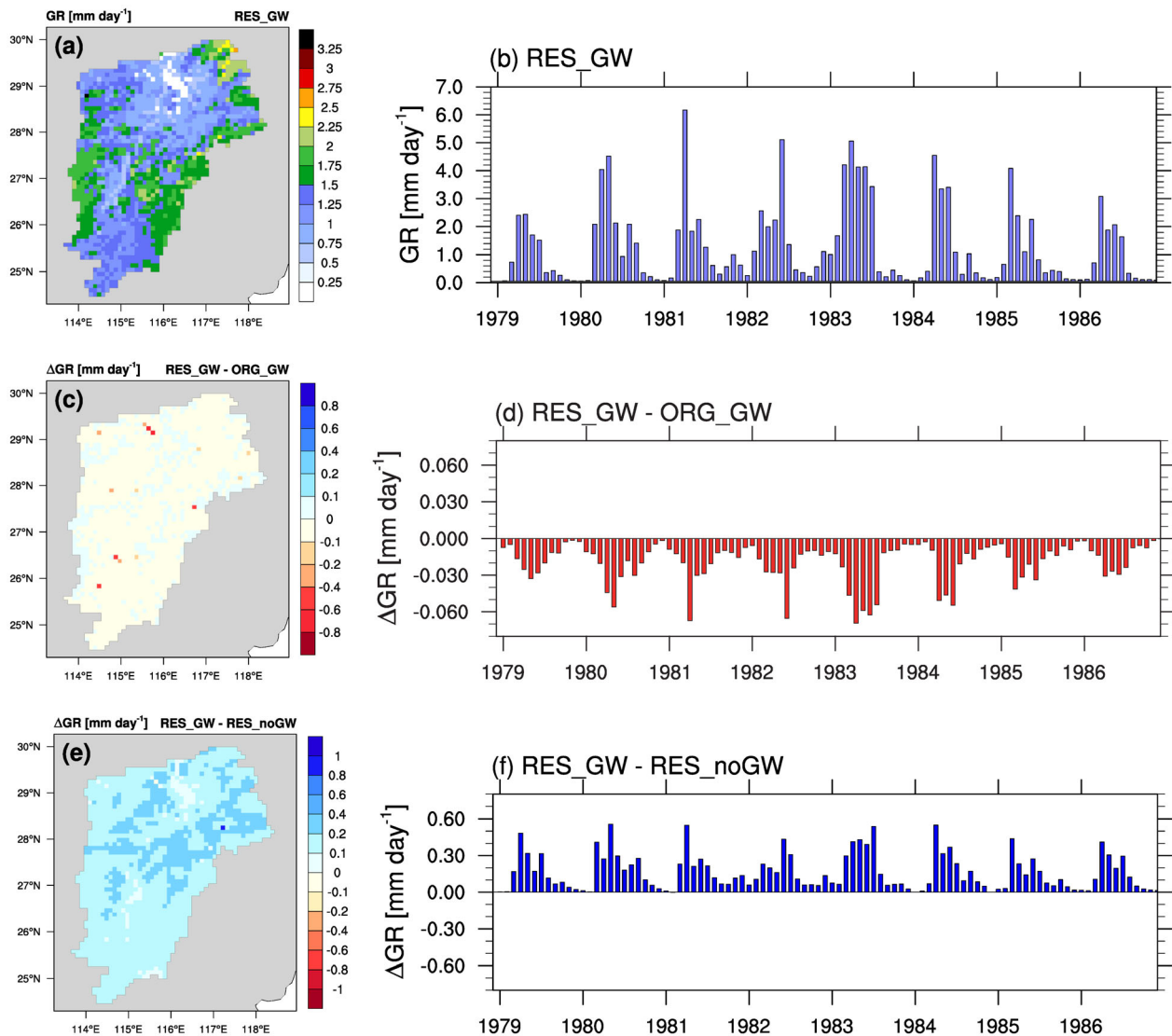
FIGURE 5 (left column) Spatial distributions of (a) the simulated groundwater recharge *GR* (mm day^{-1}) derived from the RES_GW simulation, (c) the difference in *GR* between the RES_GW simulation and the ORG_GW simulation, (e) the difference between the RES_GW simulation and the RES_noGW simulation, averaged for the period of 1979–1986. Right column shows same as the left column, but for the corresponding basin-averaged, monthly variations from 1979 to 1986

the bottom layer and the groundwater level becomes lower. Averaged over the Poyang Lake basin, −0.7% less *GR* from soils is simulated in RES_GW (Table 2).

The spatial pattern of the simulated top 1-m soil moisture *SM* in RES_GW (Figure 6(a)) shows that soil in the region adjacent to a lake (clay) is wetter than that in the southern part of the basin (clay loam). Figure 6(b) depicts that the basin-averaged monthly variation in *SM* in RES_GW has a good agreement with that derived from the reference CPC data (*r* = 0.80; *p* < 0.001 shown in Table 3).

In comparison to ORG_GW, RES_GW simulates very slightly wetter soils, mainly over the low-land river valleys (Figure 6(c)). The moistening effect of RES_GW on soils is attributed to the enhanced interactions from rivers to soils (unsaturated zone) especially in the relatively dryer months (Figure 6(d)) when water is released from reservoirs to rivers for human water-use, in connection with the

decreased recharge rates from soil water to groundwater caused by the reservoir seepage (Figure 5(d)). Averaged over the basin, the moistening effect on soils due to reservoir regulation is negligibly small.

Similar to Figure 6(a,b), Figure 7(a,b) shows the simulated surface runoff *R* in RES_GW. The comparison of the monthly time series of the basin-averaged *R* from RES_GW to that from CPC (Figure 7(b)) demonstrates that the reservoir incorporated NOAH-HMS underestimates the peaks of *R* during the rainy months, but is able to reasonably reproduce the monthly variability of *R* with a correlation coefficient of 0.93 (*p* < 0.001), but the bias in the simulated *R* is large (around −48.86%). Such underestimation of *R* could be possibly due to the overestimation of *ET* (Figure 8(b)) and *SM* (Figure 6(b)).

In comparison to ORG_GW, RES_GW simulates slightly higher values of *R* in the river valleys (Figure 7(c)), which is coherent with the

pattern of the slightly wetter soils shown in Figure 6(c). The monthly variation of the increase in R is similar to that of the groundwater

TABLE 2 Terrestrial water budget terms (mm day^{-1}) in the ORG_GW, RES_GW, RES_noGW simulations, averaged for the period of 1979–1986 for the Poyang Lake basin

	ORG_GW	RES_GW	RES_noGW
P	4.25	4.25	4.25
ET	2.24	2.30	2.35
R	0.63	0.63	0.75
ΔSM	0.01	0.01	0.02
GR	1.33	1.32	1.15
Residual	0.04	−0.01	−0.02

Note: The calculation of the residual term is based on the water balance equation $P = ET + R + \Delta SM + GR + \text{Residual}$.

recharge shown in Figure 5(d). Averaged over the basin, the increase in R due to reservoir regulation in RES_ORG is relatively small.

Figures 8(a)–10(a) and S2(a) depict the spatial patterns of the simulated evapotranspiration ET, the ET partitioning (i.e., the simulated transpiration E_t and the simulated direct evaporation E_d), and the fraction F of E_d/ET in RES_GW and Figures 8(b)–10(b) and S2(b) show the correspondingly basin-averaged monthly variations. The basin-averaged ET (Figure 8(b)) reaches the maximum value in July (the warmest month) and the minimum value in January (the coldest month), as the evapotranspiration regime for the Poyang Lake basin is energy-limited. Figure 8(b) further shows that the monthly variation of ET in RES_GW is in good agreement with that in CPC (correlation coefficient: 0.97; $p < 0.001$), but with a relative bias of around 37.38%. The comparison of E_t (Figure 9(a,b)) and E_d (Figure 10(a,b)) to ET (Figure 8(a,b)) reveals that E_t generally dominates ET in the most area of the basin (Figure S2(a)) and particularly during the warmer
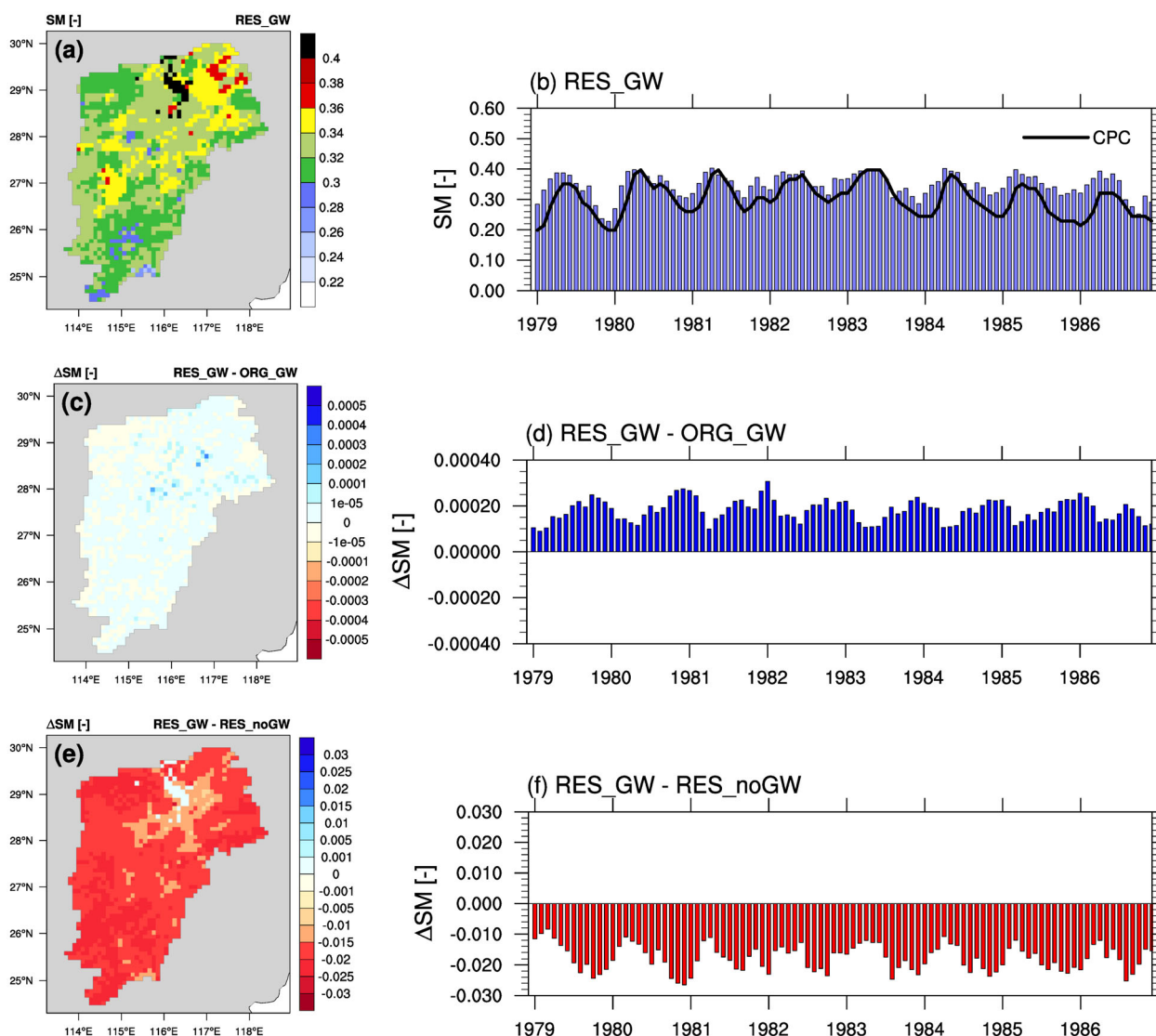

FIGURE 6 As in Figure 5, but for the simulated soil moisture SM (−) of the top 1 m. the basin-averaged, monthly time series of SM from the CPC reference data (black solid line) is additionally shown in (b) for comparison

TABLE 3 Performance measures for basin-averaged, monthly surface runoff (R), soil moisture (SM) and evapotranspiration (ET) from the RES_GW simulation against the corresponding reference data sets, averaged for different analysed periods

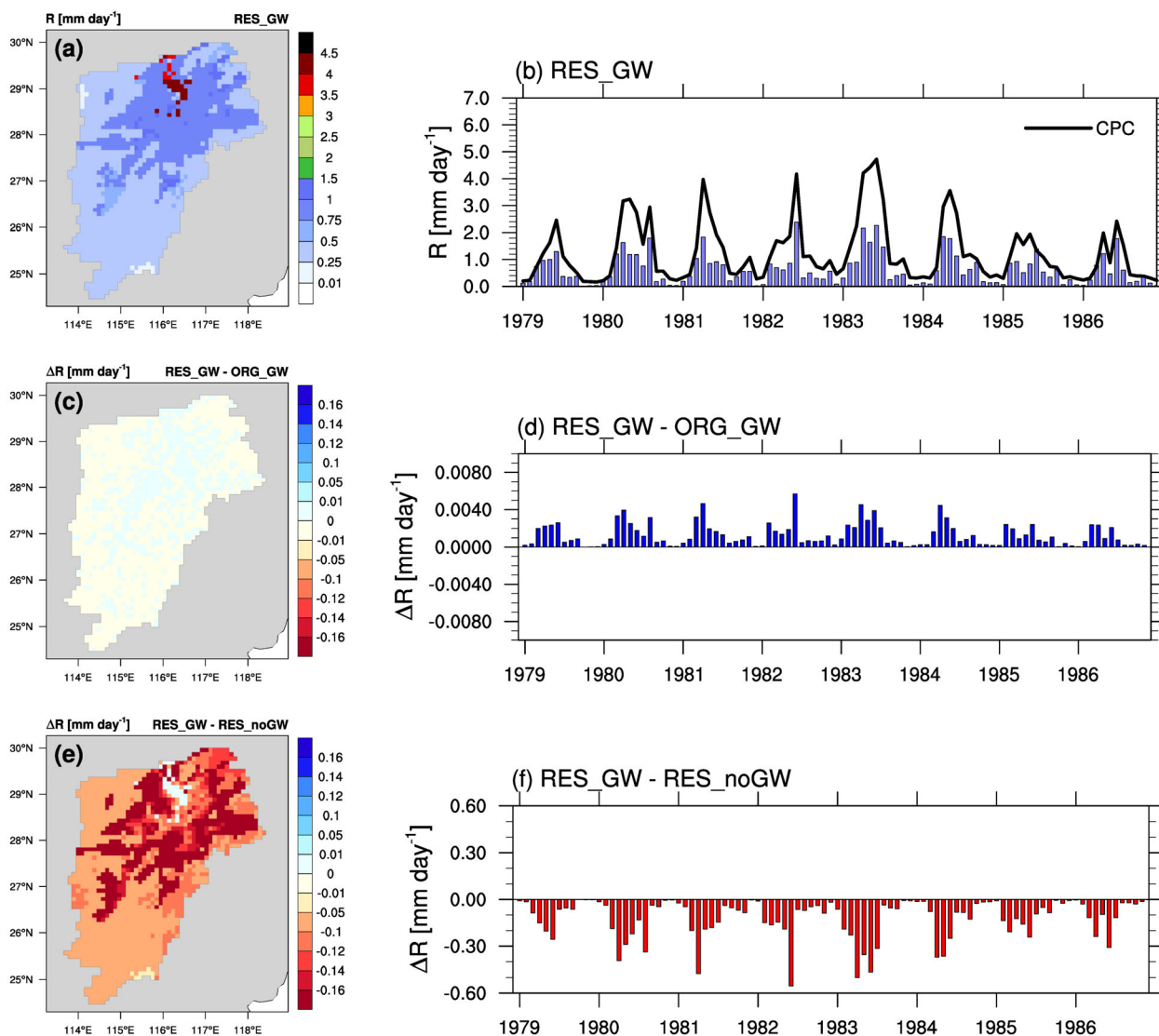|	Reference data	Analysed period	RB [%]	r [−]	NSE [−]	KGE [−]
R	CPC	1979–1986	−48.86	0.93	0.40	0.31
SM	CPC	1979–1986	15.62	0.80	−0.14	0.62
ET	CPC	1979–1986	37.38	0.97	0.71	0.59
	GLEAM	1980–1986	7.31	0.97	0.77	0.65

FIGURE 7 As in Figure 5, but for the simulated surface runoff R (mm day^{-1}). The basin-averaged, monthly time series of R from the CPC reference data (black solid line) is additionally shown in (b) for comparison

months (Figure S2(b)). Averaged over the whole basin, E_t (E_d) accounts for 64% (36%) of ET.

In comparison to ORG_GW, Figure 8(c) shows that the representation of reservoir regulation and the consideration of river evaporation in RES_GW enhance ET over the basin except for the lake area. This enhancement is higher in the regions where large-sized and medium-sized reservoirs are located and becomes negligible in the regions where small-

sized reservoirs and no river exist. For example, the maximum values of the enhanced ET (~0.75 mm day^{-1}) are found at the locations of the first two largest reservoirs of the basin (viz., Zhelin Reservoir and Wanan Reservoir). Temporally, the enhanced basin-averaged ET in RES_GW (Figure 8(d)) is found throughout the whole investigation period, with a larger enhancement in summer and smaller in winter. Averaged over the whole basin, 0.06 mm day^{-1} (+2.7%) more ET is simulated in RES_GW.
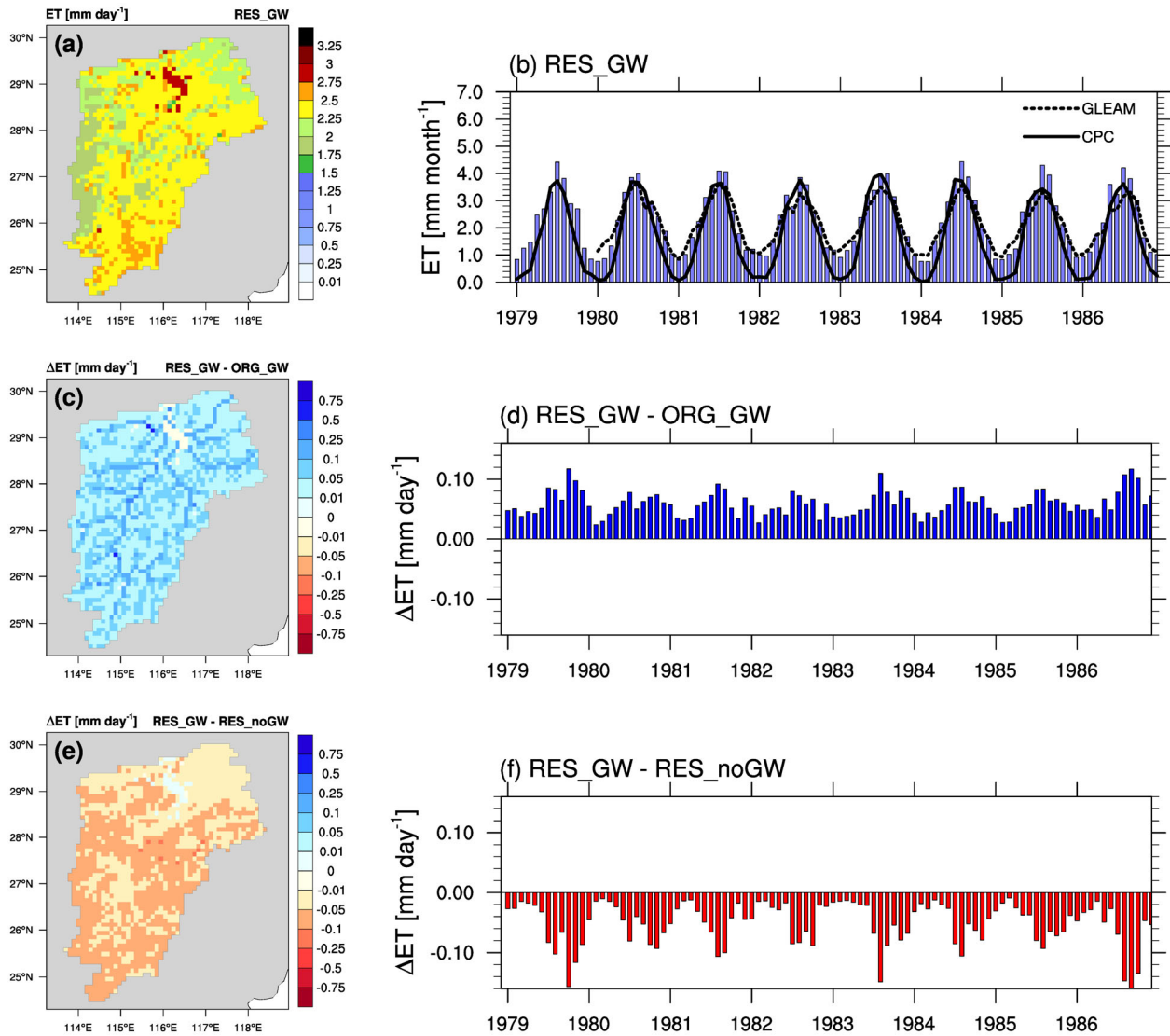
FIGURE 8 As in Figure 5, but for the simulated evapotranspiration ET (mm day^{-1}). The basin-averaged, monthly time series of ET from the CPC (black solid line) and the GLEAM (black dashed line) reference data are additionally shown in (b) for comparison

The comparison of the partitioned ET shows that the enhanced ET due to reservoir regulation in RES_GW mainly originates from the enhanced E_d (Figure 10(c,d)) and, to a very less extent, from the enhanced E_t (Figure 9(c,d)). Figure S2(c) further shows the spatial difference in the direct evaporation fraction F of E_d/ET between RES_GW and ORG_GW, revealing that locally the modified F reaches values of up to +16.3%. Averaged over the whole basin, due to reservoir regulation, the contribution of E_d (E_t) to ET in RES_GW increases (decreases) by 1.5%.

4.3 | Role of groundwater feedback in a reservoir-regulated ground-soil-vegetation continuum

To explore the role of groundwater feedback in a reservoir-regulated ground-soil-vegetation continuum, we further compare the reservoir regulation incorporated NOAH-HMS simulation with groundwater feedback (RES_GW) to the reservoir regulation incorporated NOAH-HMS simulation without groundwater feedback (RES_noGW). The spatial and temporal differences between RES_noGW and RES_GW are shown in the third rows of Figures 5–10.

In comparison to RES_noGW, the groundwater feedback-enabled RES_GW generally simulates more GR from soils (Figure 5(e,f)), less SM in the top 1-m soil (Figure 6(e,f)), decreased R at the land surface (Figure 7(e,f)), and decreased ET (E_d and E_t) to the atmosphere (Figure 8(e,f)), except over the lake. Groundwater feedback induced modifications of GR and R are similarly larger in the low-land region around the lake (Figures 5(e) and 7(e)) and during the rainy season (Figures 5(f) and 7(f)). However, the drying effect on soils decreases spatially with distance towards the lake (Figure 6(e)), and temporally with shift from summer to winter (Figure 6(f)). It is worth noting that allowing groundwater feedback modifies E_t (Figure 9(e,f)) and E_d (Figure 10(e,f)) in a different manner: the location (the timing) of the maximum decrease in E_t is found over the area of cropland (during
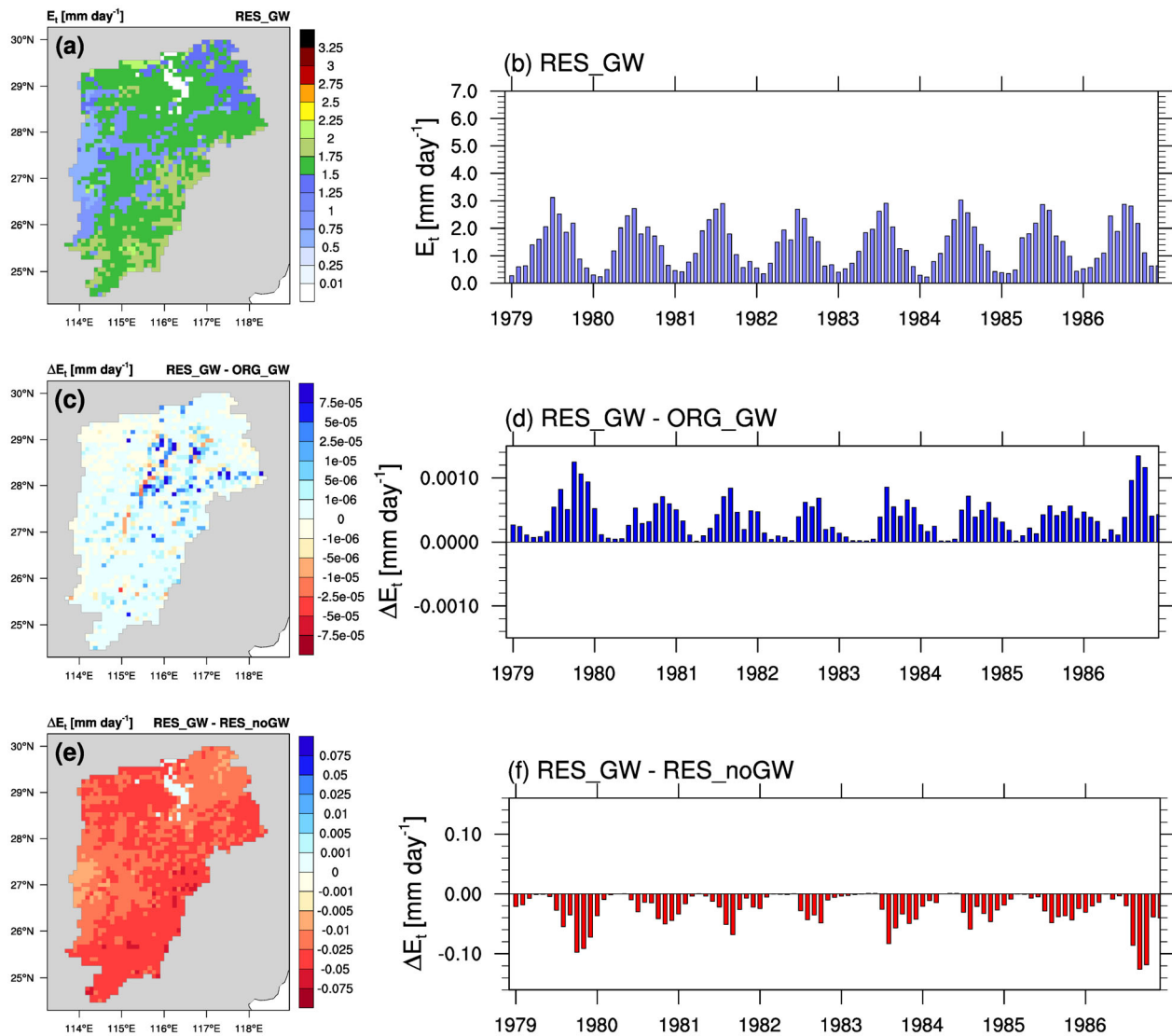
FIGURE 9 As in Figure 5, but for the simulated transpiration E_t (mm day^{-1})

the period of August–October), whereas that of the maximum decrease in E_d is found over the area of savanna (during the period of April–August). As a result, the contribution of E_d to ET in most cases decreases over the non-river pixels (Figure S2(e)) and during the summer (Figure S2(f)) by up to values of around 1.1%.

5 | DISCUSSION

5.1 | Distinct role of reservoir regulation and groundwater feedback

The previous sections quantified to what extent the simulated terrestrial water cycle for the Poyang Lake basin is modified, due to reservoir regulation (in Section 4.2) and groundwater feedback (in Section 4.3). In general, our results reveal that reservoir regulation and groundwater feedback play different roles in modification of the

simulated terrestrial water cycle of the basin. Specifically, the incorporation of reservoirs for the Poyang Lake basin decreases the basin-scale variation of the simulated streamflow (reductions of peak flow and increases in low flow), albeit to a limited extent. One reason is that the annual total water resources in the humid subtropical Poyang Lake basin are relatively high and that around 20% of the total amount is stored within the basin's reservoirs. Therefore, despite their relatively large number, the streamflow is not strongly regulated by the reservoirs. To some extent, this also explains why the inclusion of reservoir regulation into NOAH-HMS has a limited improvement on streamflow simulation for the Poyang Lake basin (in Section 4.2.1). Similar regulation effects have also been reported in numerous other studies for regions with different scales, such as, the tropical monsoon-controlled Mekong basin (Bonnema & Hossain, 2017) and the climate-varied United States continent (Gutenson et al., 2020; Shin et al., 2019). In addition to streamflow, reservoir incorporation also increases the evaporation at the land surface and modifies the
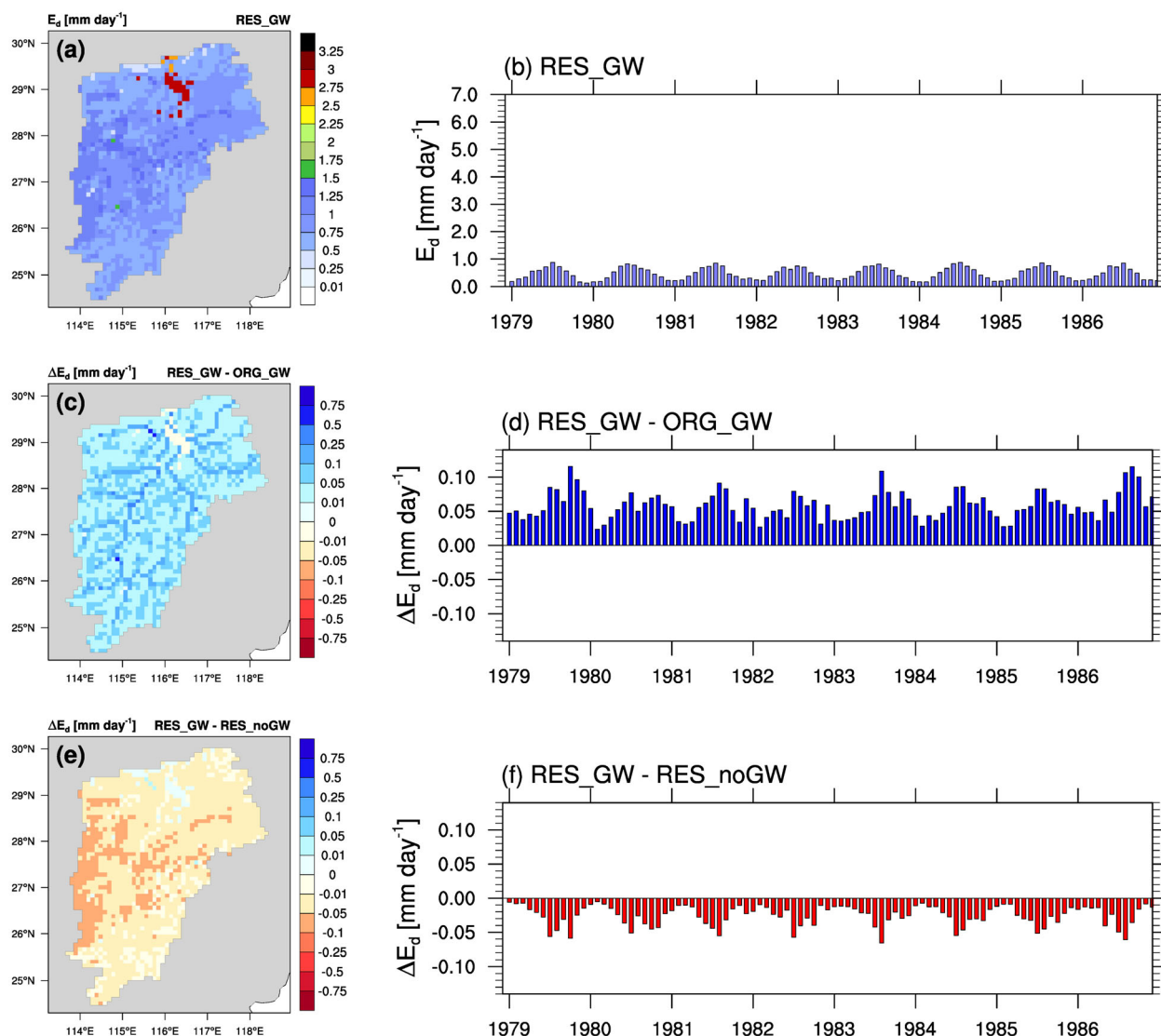
FIGURE 10 As in Figure 5, but for the simulated direct evaporation E_d (mm day^{-1})

simulated groundwater recharge from soils where reservoirs are located.

In comparison to the effects of reservoir regulation, the groundwater feedback has stronger impacts on the simulated reservoir-regulated ground-soil-vegetation continuum, especially for the simulated basin-scale surface runoff and soil moisture. Similar role of groundwater feedback has been also found in the study of Wagner et al. (2016) that did not account for reservoir regulation. This suggests that the additional representation of reservoir regulation in the NOAH-HMS modelled ground-soil-vegetation continuum does not alter the strength of the groundwater feedback for the Poyang Lake basin. This is an expected result, because many studies have revealed that the interaction between surface water and groundwater in the Poyang Lake basin is relatively strong, since the Poyang Lake basin features relatively shallow groundwater, especially in the floodplain wetland.

The connectivity between surface water and groundwater (Sophocleous, 2002) has been studied for investigations of, for

example, basin-scale water quality (Banks et al., 2011) and depletion of groundwater due to enhanced evapotranspiration (Condon et al., 2020; Maxwell & Condon, 2016). For the Poyang Lake basin, surface water–groundwater researches are, however, limited to understanding the changes in the water levels of the lake and the associated ecological changes in the surrounding flood plains and wetlands (e.g., Li et al., 2019; Liao et al., 2020). Our basin-scale study shows that groundwater feedback impacts the terrestrial water cycle of the whole basin, since the Poyang Lake basin features relatively shallow groundwater, especially in the floodplain wetland. Recent studies reveal that shallow groundwater can mitigate the warming-induced heat stress for the contiguous United States by shifting the balance between the water supply at the land surface and the water demand in the atmosphere (Condon et al., 2020; Maxwell & Condon, 2016). For our study region, the continuously increasing risk of extreme events, such as, droughts and floods, have been observed in the past (Shankman et al., 2006; Zhou et al., 2020) and is projected

to continue in the future (Sheffield et al., 2012; Wang, Guo, et al., 2017). In addition, our current and previous studies show that the reservoir regulation in the Poyang Lake basin can also mitigate the warming-induced floods (Dong, Yu, Gu, et al., 2019). In this regard, the reservoir regulation and the groundwater feedback are equally important for the Poyang Lake basin in terms of risks mitigation.

5.2 | Implications for the atmospheric water cycle

It has been well established that transpiration and direct evaporation are two distinct processes transporting water from the land surface to the atmosphere (Savenije, 2004; Shuttleworth, 2012). Recent modelling studies have revealed that the transpired water and directly evaporated water have different compositions and residence times in the atmosphere (van der Ent et al., 2014; Wang-Erlandsson et al., 2014; Wei et al., 2015, 2016). Specifically, our previous modelling study shows that the transpired water from the Poyang Lake region has a lower magnitude and resides longer in the atmospheric water cycle over Southeast China than directly evaporated water (Wei et al., 2016). In this study, our results of Sections 4.2 and 4.3 show that the reservoir regulation and the groundwater feedback in the Poyang Lake basin do not only modify the magnitude of the simulated evapotranspiration for the basin, but also change the simulated evapotranspiration partitioning (Figures 8–10). We found that the inclusion of reservoir regulation can enhance the simulated evaporation more than the simulated transpiration (Figure 10(b,e)), whereas allowing the groundwater feedback has impacts on both simulated fluxes (Figure 10(c,f)). In the context of moisture recycling (Arnault et al., 2019; Gao et al., 2020; Wei et al., 2016), the differences in partitioning the simulated evapotranspiration from the Poyang Lake basin due to reservoir regulation and due to groundwater feedback may propagate to the regionally recycled precipitation through the non-linear processes of the atmospheric water cycle.

5.3 | Uncertainties in our modelling study and perspectives

5.3.1 | Evapotranspiration estimates

Globally, the land masses provide more transpiration, that is, 61% ± 15% of evapotranspiration) than direct evaporation (Jasechko et al., 2013; Schlesinger & Jasechko, 2014), which is also the case of our modelling results for the Poyang Lake basin (Figures 7 and 8). However, it is acknowledged that uncertainties in estimates of evapotranspiration and its partitioning are considerably high due to larger uncertainties in the estimation approaches and the lack of field measurements (Coenders-Gerrits et al., 2014; Jasechko et al., 2013). To partly narrow down uncertainties associated with evapotranspiration estimates, we further analysed the GLEAM evapotranspiration product (1980–1986), in addition to CPC. With respect to the temporal variation (Figure 7(b)), the RES_GW simulated ET shows good

agreement with the GLEAM reference data ($r = 0.97$; $p < 0.001$), particularly during the non-summer period, whereas similar overestimation of ET in RES_GW is found during the summer period. Moreover, the inter-comparison of the remote sensing-based GLEAM and the model-based CPC estimates (also in Table 3) reveals that the uncertainty in their evapotranspiration estimates over the Poyang Lake basin is larger during non-summer seasons than that in summer. The lower values of the ET magnitude from CPC in comparison with these from GLEAM are partly attributed to relatively low performance of the CPC-employed one-layer 'bucket' water balance model and its adjusted Thornthwaite expression for estimating evapotranspiration (Fan & van den Dool, 2004).

5.3.2 | Partitioned evapotranspiration

Regarding evapotranspiration partitioning, we analysed the newly compiled transpiration to evapotranspiration dataset of Niu2020 for the Poyang Lake basin for 1981–1986. The comparison reveals that the spatial patterns of the annual mean direct evaporation fraction F (E_d/ET) from RES_GW and that from Niu2020 (Figure S3(a,b)) are in good agreement over the area with forests land-use type (see Figure 2(a)). It is worth to note that, for deriving evapotranspiration estimates, Niu2020 employed the Priestley–Taylor Jet Propulsion Laboratory (PT-JPL) model (Priestley & Taylor, 1972), which is different from ours, that is, the Penman–Monteith model (Monteith & Unsworth, 1990; Penman, 1948). In addition, Niu2020 was calibrated and validated against the observational evapotranspiration and the sap-flow-derived transpiration from the Qianyanzhou ChinaFLUX (forest) site in the Poyang Lake basin (see Figure S2 in Niu et al. (2020)). Therefore, we think that the uncertainty in our simulated direct evaporation fraction F over the forest area is relatively small. On the other hand, larger deviations of F are found over the irrigated area around the Poyang Lake: lower direct evaporation fraction from RES_GW in comparison with that from Niu2020, which reveals a limited capacity of our employed model in terms of representing flood-irrigation in the basin. Furthermore, the underestimation of direct evaporation fraction F around the lake area (Figure S3) and the overestimation of ET in summer (Figure 7(b)) in the RES_GW simulation reveal that our newly extended model probably overestimated transpiration rate (Figure 8(a,b)), particularly over the lake-surrounding area in summer. Such overestimation of transpiration rate in our study may be partly attributed to the Jarvis-type canopy stomatal resistance scheme (Jarvis, 1976) within our extended NOAH-HMS model framework: due to the environmental stress functions (considering solar radiation, air temperature, water vapour deficit, soil and vegetation water status and CO_2 concentration of air) in the Jarvis-type scheme (Chen & Dudhia, 2001; Noilhan & Planton, 1989), soil water can be transported by plants freely via canopy stomata especially under high temperature conditions. Numerous studies have reported similar biases of the Jarvis-type scheme simulated transpiration in different regions (Lhomme, 2001; Wang et al., 2020; Zheng et al., 2019), and suggest that, because of accounting for assimilation of CO_2 for

controlling canopy stomata, physiological-type schemes (e.g., the Ball–Berry scheme [Ball et al., 1987; Farquhar et al., 1980]) generally outperform the Jarvis-type scheme (Buckley, 2017; Fisher & Koven, 2020; Niyogi et al., 1997; Pitman, 2003). Therefore, future research on adapting our reservoir-regulation incorporated NOAH-HMS model into the NOAH-multiparameterization LSM framework (Niu et al., 2011) is needed for improving transpiration simulation and thereby likely improving representation of the terrestrial water cycle for the Poyang Lake basin.

5.3.3 | Model parameter

Reservoir seepage is one of the important water pathways within the surface–subsurface continuum, which are typically neglected due to difficulties in determining representative values for the saturated hydraulic conductivity. Often, water stable isotope signatures and laboratory-based hydraulic scale approaches are used to estimate the saturated hydraulic conductivity below reservoirs, however, these are not applicable for studies at regional scales with reservoir networks. In this study, the procedure for estimating the saturated hydraulic conductivity for 1262 reservoirs of Section 2.3 is based on seepage rates reported by the local authorities, and the spatially distributed observation-based high-resolution product of saturated hydraulic conductivity from the Chinese Geology dataset, which serves as well-defined criteria for constraining the estimated seepage of reservoirs. Therefore, we believe that, for the humid subtropical Poyang Lake basin, the uncertainties in our results originating from estimating saturated hydraulic conductivity for reservoirs are relatively small.

5.3.4 | Irrigation process

Our study region, that is, the Poyang Lake basin, is a major grain producing area for the country (Yue et al., 2019), which covers around 42% of the whole basin area (Figure 2(b)). Production of crops (e.g., double-harvest rice) in the basin requires water resources for irrigation (Ding et al., 2020; Li et al., 2012). However, our extended NOAH-HMS model does not allow to explicitly represent irrigation practices. Instead, the human water use including irrigation for reservoir operation in our study was estimated by temporally and spatially downscaling the reported basin scale annual amount for each reservoir, that has been used in numerous previous studies (e.g., Dong, Yu, Yang, et al., 2019; Yang et al., 2010). We are aware of uncertainties triggered by this simplified approach which may impact on the simulated ground-soil-vegetation continuum of our study. It is expected that such impact is scale-dependent: the magnitude of the impact at local and short-term scales is larger than that at regional and long-term scales. Moreover, it is reported by the local authorities that the irrigated water is rarely extracted from groundwater. Therefore, we assume that neglecting irrigation practices in this study will not significantly change our regional and long-term scales modelling results. Nevertheless, developing a process-based irrigation scheme (e.g., Qian

et al., 2013) in the framework of a fully coupled atmospheric–hydrologic modelling system is an on-going research activity.

5.3.5 | Model resolution

Our study is based on simulations with a spatial resolution of 10 km, because NOAH-HMS, the basic model used for the implementation of a reservoir regulation scheme, is designed for hydrologic applications at regional and long-term scales (Wagner et al., 2016; Yu et al., 2006). At these scales (i.e., 10 km), the parameterized reservoir regulation processes for the considered reservoirs in this study are mostly sub-grid scale processes (Yu, 2000). It is well-known that scale issues exits in hydrological modelling (Blöschl & Sivapalan, 1995), which means that the extents of the modified terrestrial water cycle for the Poyang Lake basin due to the inclusion of reservoir regulation may vary with changes in spatial resolution of simulations (Famiglietti & Wood, 1995; Shrestha et al., 2015, 2018). Furthermore, the strategy of implementation of reservoir regulation proposed in this study (Section 2.3) can also be adapted to state-of-art fully coupled atmospheric–hydrologic modelling systems, such as, WRF-Hydro (Rummler et al., 2019; Senatore et al., 2015), TerrSysMP (Kurtz et al., 2016; Shrestha et al., 2014) and ParFlow.WRF (Maxwell et al., 2011). In comparison with NOAH-HMS, the hydrologic components of these modelling systems are more complex and, with the extension of a reservoir module, thereby are more suitable for practical purposes (e.g., optimal operation of multi-reservoir system) at local and real-time scales.

5.3.6 | Study period

In this study, our analyses are restricted to the period of 1978–1986 due to data availability. The selection of this study period, however, allows us to compare our results directly with those from Wagner et al. (2016) (see Section 5.1). Regarding the recent changes in our results, we think that changes in the parameterized reservoirs across time are rather small due to the fact that most of the reservoirs in the Poyang Lake basin were constructed before the 1980s. We also expect that the identified feedback mechanism between surface water and groundwater on the basin scale across time is not noticeably altered due to the facts that the climate of the Poyang Lake basin is characterized as humid subtropical and the irrigated water in the basin is rarely extracted from groundwater. However, observational and modelling studies showed that climate change has changed the hydrologic regime in the Poyang Lake basin over the last decades, such as runoff variations (Lei et al., 2021; Ye et al., 2013), extreme temperature and precipitation (Zhang et al., 2016), and flash floods and -droughts (Li et al., 2014; Zhou et al., 2020). These changes could likely affect our results to some extent, as for example, the changes in the simulated evaporation of reservoirs on seasonal scale which is induced by changed runoff and/or precipitation variations. Future studies in this direction could be conducted with our modelling framework for a quantitative analysis.

6 | SUMMARY AND CONCLUSIONS

In this study, the reservoir regulation module of Dong, Yu, Gu, et al. (2019) has been implemented into the terrestrial component, that is, the NOAH-HMS, of the fully coupled atmospheric–hydrologic modelling system WRF-HMS (Wagner et al., 2016). This implementation allows to represent human-induced reservoir regulation processes in the terrestrial water cycle and later has repercussions on the atmospheric water cycle.

The reservoir regulation-incorporated, two-way coupled surface water–groundwater model NOAN-HMS has been applied to the Poyang Lake basin of China, with a large number of reservoirs and a strong surface water–groundwater interaction. Using the extended model, the impact of the incorporated reservoir regulation module in terms of simulating streamflow and the modification of the simulated terrestrial water cycle for the Poyang Lake basin during 1979–1986 were investigated. In addition, the role of groundwater feedback in the simulated reservoir-regulated ground-soil-vegetation continuum for the Poyang Lake basin was assessed as well.

Our main results are summarized as follows:

1. For the 8 years period of 1979–1986, the results of the model evaluation show that the inclusion of reservoir regulation in the NOAH-HMS model slightly improves the streamflow simulation at daily and monthly scale for the Poyang Lake basin, particularly for the comparatively large sub-basins where more reservoirs exist. In addition, the reservoir regulation incorporated NOAH-HMS has a reasonable performance on reproducing the monthly variations in the basin-averaged surface runoff, soil moisture and evapotranspiration derived from the gridded CPC reference data.

2. Regarding the modification of the simulated natural terrestrial water cycle for the Poyang Lake basin, averaged over the whole basin and for the whole investigated period, the reservoir regulation leads to very slightly lower groundwater recharge from soils, wetter soils, more runoff, but leads to largely increased evapotranspiration (mainly evaporation). Such modifications may vary and become larger at the local scale.

3. Our performed sensitivity analysis reveals that allowing the groundwater feeding back to the soil water does modify the simulated reservoir-regulated groundwater-soil-vegetation continuum: higher groundwater recharge, dryer soils, lower surface runoff, and decreased evapotranspiration, irrespective of the reservoir regulation.

In conclusion, the results of the performed sensitivity analysis give evidence that reservoir regulation and groundwater feedback play different roles in modifying the regional terrestrial water cycle for the Poyang Lake basin, particularly with respect to the partitioning of the simulated evapotranspiration. The implementation of reservoir regulation into the terrestrial component (i.e., NOAH-HMS) of the fully coupled atmospheric–hydrological modelling system, that is, the WRF-HMS (Wagner et al., 2016) allows us moving one step further towards representation of complex, dynamic reservoir regulation processes in the full water cycle, which has been emphasized by the community (Friedrich et al., 2018).

In the future, we will address how reservoir regulation modifies the atmospheric water cycle using the fully coupled, regional atmospheric–hydrologic model system WRF-HMS. In addition, the reservoir regulation represented modelling framework established in this study could be extended further to account for water withdrawals from reservoirs water and/or groundwater and to account for irrigation activities for future studies of assessing irrigation effects on the water cycle.

DATA AVAILABILITY STATEMENT

The data from the modeling that support the findings of this study are stored in KIT/IMK-IFU and are available from the corresponding author upon request.

ORCID

Jianhui Wei https://orcid.org/0000-0001-8609-9600
Ningpeng Dong https://orcid.org/0000-0002-5226-6180
Benjamin Fersch https://orcid.org/0000-0002-4660-1165
Joël Arnault https://orcid.org/0000-0001-8859-5173
Zhenyu Zhang https://orcid.org/0000-0002-9155-7378
Chuanguo Yang https://orcid.org/0000-0003-1751-2160
Lu Gao https://orcid.org/0000-0003-1934-5802

REFERENCES

Adam, J. C., Haddeland, I., Su, F., & Lettenmaier, D. P. (2007). Simulation of reservoir influences on annual and seasonal streamflow changes for the Lena, Yenisei, and Ob' rivers. *Journal of Geophysical Research Atmospheres*, 112, 1–22. https://doi.org/10.1029/2007JD008525

Arnault, J., Rummler, T., Baur, F., Lerch, S., Wagner, S., Fersch, B., Zhang, Z., Kerandi, N., Keil, C., & Kunstmann, H. (2018). Precipitation sensitivity to the uncertainty of terrestrial water flow in WRF-hydro:

An ensemble analysis for Central Europe. *Journal of Hydrometeorology*, *19*(6), 1007–1025. https://doi.org/10.1175/JHM-D-17-0042.1

Arnault, J., Wagner, S., Rummler, T., Fersch, B., Bliefernicht, J., Andresen, S., & Kunstmann, H. (2016). Role of runoff–infiltration partitioning and resolved overland flow on land–atmosphere feedbacks: A case study with the WRF-hydro coupled modeling system for West Africa. *Journal of Hydrometeorology*, *17*(5), 1489–1516. https://doi.org/10.1175/JHM-D-15-0089.1

Arnault, J., Wei, J., Rummler, T., Fersch, B., Zhang, Z., Jung, G., Wagner, S., & Kunstmann, H. (2019). A joint soil-vegetation-atmospheric water tagging procedure with WRF-hydro: Implementation and application to the case of precipitation partitioning in the upper Danube River basin. *Water Resources Research*, *55*(7), 6217–6243. https://doi.org/10.1029/2019WR024780

Ball, J. T., Woodrow, I. E., & Berry, J. A. (1987). A model predicting stomatal conductance and its contribution to the control of photosynthesis under different environmental conditions. In *Progress in photosynthesis research* (pp. 221–224). Springer Netherlands. https://doi.org/10.1007/978-94-017-0519-6-48

Banks, E. W., Simmons, C. T., Love, A. J., & Shand, P. (2011). Assessing spatial and temporal connectivity between surface water and groundwater in a regional catchment: Implications for regional scale water quantity and quality. *Journal of Hydrology*, *404*, 30–49. https://doi.org/10.1016/j.jhydrol.2011.04.017

Barthel, R., & Banzhaf, S. (2016). Groundwater and surface water interaction at the regional-scale – A review with focus on regional integrated models. *Water Resources Management*, *30*, 1–32. https://doi.org/10.1007/s11269-015-1163-z

Biemans, H., Haddeland, I., Kabat, P., Ludwig, F., Hutjes, R. W. A., Heinke, J., von Bloh, W., & Gerten, D. (2011). Impact of reservoirs on river discharge and irrigation water supply during the 20th century. *Water Resources Research*, *47*, 1–15. https://doi.org/10.1029/2009WR008929

Blöschl, G., & Sivapalan, M. (1995). Scale issues in hydrological modelling: A review. *Hydrological Processes*, *9*, 251–290. https://doi.org/10.1002/hyp.3360090305

Bonnema, M., & Hossain, F. (2017). Inferring reservoir operating patterns across the Mekong Basin using only space observations. *Water Resources Research*, *53*, 3791–3810. https://doi.org/10.1002/2016WR019978

Brunner, P., & Simmons, C. T. (2012). HydroGeoSphere: A fully integrated, physically based hydrological model. *Ground Water*, *50*, 170–176. https://doi.org/10.1111/j.1745-6584.2011.00882.x

Buckley, T. N. (2017). Modeling stomatal conductance. *Plant Physiology*, *174*, 572–582. https://doi.org/10.1104/pp.16.01772

Chen, F., & Dudhia, J. (2001). Coupling an advanced land surface–hydrology model with the Penn State–NCAR MM5 modeling system. Part I: Model implementation and sensitivity. *Monthly Weather Review*, *129*(4), 569–585. https://doi.org/10.1175/1520-0493(2001)129<0587:CAALSH>2.0.CO;2

Claussen, M., Mysak, L., Weaver, A., Crucifix, M., Fichefet, T., Loutre, M. F., Weber, S., Alcamo, J., Alexeev, V., Berger, A., Calov, R., Ganopolski, A., Goosse, H., Lohmann, G., Lunkeit, F., Mokhov, I., Petoukhov, V., Stone, P., & Wang, Z. (2002). Earth system models of intermediate complexity: Closing the gap in the spectrum of climate system models. *Climate Dynamics*, *18*, 579–586. https://doi.org/10.1007/s00382-001-0200-1

Coenders-Gerrits, A. M. J., van der Ent, R. J., Bogaard, T. A., Wang-Erlandsson, L., Hrachowitz, M., & Savenije, H. H. G. (2014). Uncertainties in transpiration estimates. *Nature*, *506*(7487), E1–E2. https://doi.org/10.1038/nature12925

Condon, L. E., Atchley, A. L., & Maxwell, R. M. (2020). Evapotranspiration depletes groundwater under warming over the contiguous United States. *Nature Communications*, *11*, 873. https://doi.org/10.1038/s41467-020-14688-0

Condon, L. E., & Maxwell, R. M. (2014). Groundwater-fed irrigation impacts spatially distributed temporal scaling behavior of the natural system: A spatio-temporal framework for understanding water management impacts. *Environmental Research Letters*, *9*, 034009. https://doi.org/10.1088/1748-9326/9/3/034009

Dang, T. D., Chowdhury, A. F. M. K., & Galelli, S. (2020). On the representation of water reservoir storage and operations in large-scale hydrological models: Implications on model parameterization and climate change impact assessments. *Hydrology and Earth System Sciences*, *24*, 397–416. https://doi.org/10.5194/hess-24-397-2020

Darcy, H. (1856). *Les fontaines publiques de la ville de Dijon*. Recherche.

de Rooij, G. H. (2010). Comments on "improving the numerical simulation of soil moisture-based Richards equation for land models with a deep or shallow water table". *Journal of Hydrometeorology*, *11*(4), 1044–1050. https://doi.org/10.1175/2010JHM1189.1

Ding, M., Guan, Q., Li, L., Zhang, H., Liu, C., & Zhang, L. (2020). Phenology-based rice paddy mapping using multi-source satellite imagery and a fusion algorithm applied to the Poyang Lake plain, Southern China. *Remote Sensing*, *12*, 1022. https://doi.org/10.3390/rs12061022

Ding, Y., & Chan, J. C. L. (2005). The east Asian summer monsoon: An overview. *Meteorology and Atmospheric Physics*, *89*(1–4), 117–142. https://doi.org/10.1007/s00703-005-0125-z

Döll, P., Fiedler, K., & Zhang, J. (2009). Global-scale analysis of river flow alterations due to water withdrawals and reservoirs. *Hydrology and Earth System Sciences*, *13*, 2413–2432. https://doi.org/10.5194/hess-13-2413-2009

Dong, N., Yang, M., Yu, Z., Wei, J., Yang, C., Yang, Q., Liu, X., Lei, X., Wang, H., & Kunstmann, H. (2020). Water resources management in a reservoir-regulated basin: Implications of reservoir network layout on streamflow and hydrologic alteration. *Journal of Hydrology*, *586*, 124903. https://doi.org/10.1016/j.jhydrol.2020.124903

Dong, N., Yu, Z., Gu, H., Yang, C., Yang, M., Wei, J., Wang, H., Arnault, J., Laux, P., & Kunstmann, H. (2019). Climate-induced hydrological impact mitigated by a high-density reservoir network in the Poyang Lake Basin. *Journal of Hydrology*, *579*, 124148. https://doi.org/10.1016/j.jhydrol.2019.124148

Dong, N., Yu, Z., Yang, C., Yang, M., & Wang, W. (2019). Hydrological impact of a reservoir network in the upper Gan River basin, China. *Hydrological Processes*, *33*, 1709–1723. https://doi.org/10.1002/hyp.13433

Ehsani, N., Vörösmarty, C. J., Fekete, B. M., & Stakhiv, E. Z. (2017). Reservoir operations under climate change: Storage capacity options to mitigate risk. *Journal of Hydrology*, *555*, 435–446. https://doi.org/10.1016/j.jhydrol.2017.09.008

Famiglietti, J. S., & Wood, E. F. (1995). Effects of spatial variability and scale on areally averaged evapotranspiration. *Water Resources Research*, *31*(3), 699–712. https://doi.org/10.1029/94WR02820

Fan, Y., & van den Dool, H. (2004). Climate Prediction Center global monthly soil moisture data set at 0.5° resolution for 1948 to present. *Journal of Geophysical Research D: Atmospheres*, *109*, 1–8. https://doi.org/10.1029/2003JD004345

Farquhar, G. D., von Caemmerer, S., & Berry, J. A. (1980). A biochemical model of photosynthetic CO_2 assimilation in leaves of C3 species. *Planta*, *149*(1), 78–90. https://doi.org/10.1007/BF00386231

Feng, L., Hu, C., Chen, X., Cai, X., Tian, L., & Gan, W. (2012). Assessment of inundation changes of Poyang Lake using MODIS observations between 2000 and 2010. *Remote Sensing of Environment*, *121*, 80–92. https://doi.org/10.1016/j.rse.2012.01.014

Feng, W., Mariotte, P., Xu, L., Buttler, A., Bragazza, L., Jiang, J., & Santonja, M. (2020). Seasonal variability of groundwater level effects on the growth of *Carex cinerascens* in lake wetlands. *Ecology and Evolution*, *10*, 517–526. https://doi.org/10.1002/ece3.5926

Fersch, B., & Kunstmann, H. (2014). Atmospheric and terrestrial water budgets: Sensitivity and performance of configurations and global

driving data for long term continental scale WRF simulations. *Climate Dynamics*, *42*(9–10), 2367–2396. https://doi.org/10.1007/s00382-013-1915-5

Fersch, B., Senatore, A., Adler, B., Arnault, J., Mauder, M., Schneider, K., Völksch, I., & Kunstmann, H. (2020). High-resolution fully coupled atmospheric-hydrological modeling: A cross-compartment regional water and energy cycle evaluation. *Hydrology and Earth System Sciences*, *24*, 2457–2481. https://doi.org/10.5194/hess-24-2457-2020

Fersch, B., Wagner, S., Rummler, T., Gochis, D., & Kunstmann, H. (2013). Impact of groundwater dynamics and soil-type on modelling coupled water exchange processes between land and atmosphere. *IAHS Publication*, *359*, 140–145. http://cat.inist.fr/?aModele=afficheN&cpsidt=27916731

Fisher, R. A., & Koven, C. D. (2020). Perspectives on the future of land surface models and the challenges of representing complex terrestrial systems. *Journal of Advances in Modeling Earth Systems*, *12*, 1–24. https://doi.org/10.1029/2018MS001453

Flato, G. M. (2011). Earth system models: An overview. *Wiley Interdisciplinary Reviews: Climate Change*, *2*(6), 783–800. https://doi.org/10.1002/wcc.148

Friedrich, K., Grossman, R. L., Huntington, J., Blanken, P. D., Lenters, J., Holman, K. L. D., Gochis, D., Livneh, B., Prairie, J., Skeie, E., Healey, N. C., Dahm, K., Pearson, C., Finnessey, T., Hook, S. J., & Kowalski, T. (2018). Reservoir evaporation in the Western United States. *Bulletin of the American Meteorological Society*, *99*, 167–187. https://doi.org/10.1175/BAMS-D-15-00224.1

Gao, Y., Chen, F., Miguez-Macho, G., & Li, X. (2020). Understanding precipitation recycling over the Tibetan plateau using tracer analysis with WRF. *Climate Dynamics*, *55*, 2921–2937. https://doi.org/10.1007/s00382-020-05426-9

Gu, C., Mu, X., Gao, P., Zhao, G., Sun, W., & Li, P. (2017). Effects of climate change and human activities on runoff and sediment inputs of the largest freshwater lake in China, Poyang Lake. *Hydrological Sciences Journal*, *62*, 2313–2330. https://doi.org/10.1080/02626667.2017.1372856

Gudmundsson, L., Boulange, J., Do, H. X., Gosling, S. N., Grillakis, M. G., Koutroulis, A. G., Leonard, M., Liu, J., Müller Schmied, H., Papadimitriou, L., Pokhrel, Y., Seneviratne, S. I., Satoh, Y., Thiery, W., Westra, S., Zhang, X., & Zhao, F. (2021). Globally observed trends in mean and extreme river flow attributed to climate change. *Science*, *371*(6534), 1159–1162. https://doi.org/10.1126/science.aba3996

Guimberteau, M., Laval, K., Perrier, A., & Polcher, J. (2012). Global effect of irrigation and its impact on the onset of the Indian summer monsoon. *Climate Dynamics*, *39*, 1329–1348. https://doi.org/10.1007/s00382-011-1252-5

Gupta, H. V., Kling, H., Yilmaz, K. K., & Martinez, G. F. (2009). Decomposition of the mean squared error and NSE performance criteria: Implications for improving hydrological modelling. *Journal of Hydrology*, *377*, 80–91. https://doi.org/10.1016/j.jhydrol.2009.08.003

Gutenson, J., Tavakoly, A., Wahl, M., & Follum, M. (2020). Comparison of generalized non-data-driven lake and reservoir routing models for global-scale hydrologic forecasting of reservoir outflow at diurnal time steps. *Hydrology and Earth System Sciences*, *24*, 2711–2729. https://doi.org/10.5194/hess-24-2711-2020

Haddeland, I., Heinke, J., Biemans, H., Eisner, S., Flörke, M., Hanasaki, N., Konzmann, M., Ludwig, F., Masaki, Y., Schewe, J., Stacke, T., Tessler, Z. D., Wada, Y., & Wisser, D. (2014). Global water resources affected by human interventions and climate change. *Proceedings of the National Academy of Sciences of the United States of America*, *111*, 3251–3256. https://doi.org/10.1073/pnas.1222475110

Haddeland, I., Skaugen, T., & Lettenmaier, D. P. (2006). Anthropogenic impacts on continental surface water fluxes. *Geophysical Research Letters*, *33*, 1–4. https://doi.org/10.1029/2006GL026047

Hanasaki, N., Kanae, S., Oki, T., Masuda, K., Motoya, K., Shirakawa, N., Shen, Y., & Tanaka, K. (2008a). An integrated model for the

assessment of global water resources – Part 1: Model description and input meteorological forcing. *Hydrology and Earth System Sciences*, *12*, 1007–1025. https://doi.org/10.5194/hess-12-1007-2008

Hanasaki, N., Kanae, S., Oki, T., Masuda, K., Motoya, K., Shirakawa, N., Shen, Y., & Tanaka, K. (2008b). An integrated model for the assessment of global water resources – Part 2: Applications and assessments. *Hydrology and Earth System Sciences*, *12*, 1027–1037. https://doi.org/10.5194/hess-12-1027-2008

Hoang, L. P., van Vliet, M. T. H., Kummu, M., Lauri, H., Koponen, J., Supit, I., Leemans, R., Kabat, P., & Ludwig, F. (2019). The Mekong's future flows under multiple drivers: How climate change, hydropower developments and irrigation expansions drive hydrological changes. *Science of the Total Environment*, *649*, 601–609. https://doi.org/10.1016/j.scitotenv.2018.08.160

Huntington, J. L., & Niswonger, R. G. (2012). Role of surface-water and groundwater interactions on projected summertime streamflow in snow dominated regions: An integrated modeling approach. *Water Resources Research*, *48*, 1–20. https://doi.org/10.1029/2012WR012319

Huntington, T. G. (2006). Evidence for intensification of the global water cycle: Review and synthesis. *Journal of Hydrology*, *319*(1–4), 83–95. https://doi.org/10.1016/j.jhydrol.2005.07.003

Im, E.-S., & Eltahir, E. A. B. (2014). Enhancement of rainfall and runoff upstream from irrigation location in a climate model of West Africa. *Water Resources Research*, *50*(11), 8651–8674. https://doi.org/10.1002/2014WR015592

Jaramillo, F., & Destouni, G. (2015). Local flow regulation and irrigation raise global human water consumption and footprint. *Science*, *350*, 1248–1251. https://doi.org/10.1126/science.aad1010

Jarvis, P. G. (1976). The interpretation of the variations in leaf water potential and stomatal conductance found in canopies in the field. *Philosophical Transactions of the Royal Society B: Biological Sciences*, *273*(927), 593–610. https://doi.org/10.1098/rstb.1976.0035

Jasechko, S., Sharp, Z. D., Gibson, J. J., Birks, S. J., Yi, Y., & Fawcett, P. J. (2013). Terrestrial water fluxes dominated by transpiration. *Nature*, *496*(7445), 347–350. https://doi.org/10.1038/nature11983

Jiang, H., Simonovic, S. P., Yu, Z., & Wang, W. (2020). A system dynamics simulation approach for environmentally friendly operation of a reservoir system. *Journal of Hydrology*, *587*, 124971. https://doi.org/10.1016/j.jhydrol.2020.124971

Keune, J., Sulis, M., Kollet, S., Siebert, S., & Wada, Y. (2018). Human water use impacts on the strength of the continental sink for atmospheric water. *Geophysical Research Letters*, *45*, 4068–4076. https://doi.org/10.1029/2018GL077621

Kling, H., Fuchs, M., & Paulin, M. (2012). Runoff conditions in the upper Danube basin under an ensemble of climate change scenarios. *Journal of Hydrology*, *424–425*, 264–277. https://doi.org/10.1016/j.jhydrol.2012.01.011

Knoben, W. J. M., Freer, J. E., & Woods, R. A. (2019). Technical note: Inherent benchmark or not? Comparing Nash-Sutcliffe and Kling-Gupta efficiency scores. *Hydrology and Earth System Sciences*, *23*, 4323–4331. https://doi.org/10.5194/hess-23-4323-2019

Kurtz, W., He, G., Kollet, S. J., Maxwell, R. M., Vereecken, H., & Franssen, H. J. H. (2016). TerrSysMP-PDAF (version 1.0): A modular high-performance data assimilation framework for an integrated land surface-subsurface model. *Geoscientific Model Development*, *9*, 1341–1360. https://doi.org/10.5194/gmd-9-1341-2016

Laux, P., Nguyen, P. N. B., Cullmann, J., Van, T. P., & Kunstmann, H. (2016). How many RCM ensemble members provide confidence in the impact of land-use land cover change? *International Journal of Climatology*, *37*, 2080–2100. https://doi.org/10.1002/joc.4836

Lei, X., Gao, L., Wei, J., Ma, M., Xu, L., Fan, H., Li, X., Gao, J., Dang, H., Chen, X., & Fang, W. (2021). Contributions of climate change and human activities to runoff variations in the Poyang Lake Basin of China. *Physics and Chemistry of the Earth, Parts A/B/C*, *123*, 103019. https://doi.org/10.1016/j.pce.2021.103019

Lhomme, J. P. (2001). Stomatal control of transpiration: Examination of the Jarvis-type representation of canopy resistance in relation to humidity. *Water Resources Research*, 37, 689–699. https://doi.org/10.1029/2000WR900324

Li, P., Feng, Z., Jiang, L., Liu, Y., & Xiao, X. (2012). Changes in rice cropping systems in the Poyang Lake region, China during 2004–2010. *Journal of Geographical Sciences*, 22(4), 653–668. https://doi.org/10.1007/s11442-012-0954-x

Li, X., Zhang, Q., Xu, C.-Y., & Ye, X. (2014). The changing patterns of floods in Poyang Lake, China: Characteristics and explanations. *Natural Hazards*, 76(1), 651–666. https://doi.org/10.1007/s11069-014-1509-5

Li, X., Cheng, G., Ge, Y., Li, H., Han, F., Hu, X., ... Cai, X. (2018). Hydrological cycle in the Heihe River Basin and its implication for water resource management in endorheic basins. *Journal of Geophysical Research: Atmospheres*. 123(2), 890–914. https://doi.org/10.1002/2017JD027889

Li, Y., Zhang, Q., Lu, J., Yao, J., & Tan, Z. (2019). Assessing surface water–groundwater interactions in a complex river-floodplain wetland-isolated lake system. *River Research and Applications*, 35, 25–36. https://doi.org/10.1002/rra.3389

Liao, F., Wang, G., Yi, L., Shi, Z., Cheng, G., Kong, Q., Mu, W., Guo, L., Cheng, K., Dong, N., & Liu, C. (2020). Identifying locations and sources of groundwater discharge into Poyang Lake (eastern China) using radium and stable isotopes (deuterium and oxygen-18). *Science of the Total Environment*, 740, 140163. https://doi.org/10.1016/j.scitotenv.2020.140163

Liu, X., Yang, M., Meng, X., Wen, F., & Sun, G. (2019). Assessing the impact of reservoir parameters on runoff in the Yalong River basin using the SWAT model. *Water*, 11, 1–20. https://doi.org/10.3390/w11040643

Liu, Y., Wu, G., & Zhao, X. (2013). Recent declines in China's largest freshwater lake: Trend or regime shift? *Environmental Research Letters*, 8(1), 014010. https://doi.org/10.1088/1748-9326/8/1/014010

Lv, M., Hao, Z., Lin, Z., Ma, Z., Lv, M., & Wang, J. (2016). Reservoir operation with feedback in a coupled land surface and hydrologic model: A case study of the Huai River basin, China. *JAWRA Journal of the American Water Resources Association*, 52(1), 168–183. https://doi.org/10.1111/1752-1688.12375

Mahrt, L., & Ek, M. (1984). The influence of atmospheric stability on potential evaporation. *Journal of Climate & Applied Meteorology*, 23, 222–234. https://doi.org/10.1175/1520-0450(1984)023<0222:TIOASO>2.0.CO;2

Maxwell, R. M., & Condon, L. E. (2016). Connections between groundwater flow and transpiration partitioning. *Science*, 353(6297), 377–380.

Maxwell, R. M., Lundquist, J. K., Mirocha, J. D., Smith, S. G., Woodward, C. S., & Tompson, A. F. B. (2011). Development of a coupled groundwater–atmosphere model. *Monthly Weather Review*, 139, 96–116. https://doi.org/10.1175/2010MWR3392.1

Maxwell, R. M., Putti, M., Meyerhoff, S., Delfs, J. O., Ferguson, I. M., Ivanov, V., Kim, J., Kolditz, O., Kollet, S. J., Kumar, M., Lopez, S., Niu, J., Paniconi, C., Park, Y. J., Phanikumar, M. S., Shen, C., Sudicky, E. A., & Sulis, M. (2014). Surface-subsurface model intercomparison: A first set of benchmark results to diagnose integrated hydrology and feedbacks. *Water Resources Research*, 50, 1531–1549. https://doi.org/10.1002/2013WR013725

Melsen, L. A., Teuling, A. J., Torfs, P. J. J. F., Uijlenhoet, R., Mizukami, N., & Clark, M. P. (2016). HESS opinions: The need for process-based evaluation of large-domain hyper-resolution models. *Hydrology and Earth System Sciences*, 20(3), 1069–1079. https://doi.org/10.5194/hess-20-1069-2016

Miralles, D. G., Holmes, T. R. H., De Jeu, R. A. M., Gash, J. H., Meesters, A. G. C. A., & Dolman, A. J. (2011). Global land-surface evaporation estimated from satellite-based observations. *Hydrology and Earth System Sciences*, 15(2), 453–469. https://doi.org/10.5194/hess-15-453-2011

Monteith, J. L., & Unsworth, M. H. (1990). *Principles of environmental physics* (2nd ed.). Edward Arnold.

Nash, J. E., & Sutcliffe, J. V. (1970). River flow forecasting through conceptual models part I – A discussion of principles. *Journal of Hydrology*, 10, 282–290. https://doi.org/10.1016/0022-1694(70)90255-6

Nazemi, A., & Wheater, H. S. (2015a). On inclusion of water resource management in earth system models – Part 1: Problem definition and representation of water demand. *Hydrology and Earth System Sciences*, 19, 33–61. https://doi.org/10.5194/hess-19-33-2015

Nazemi, A., & Wheater, H. S. (2015b). On inclusion of water resource management in earth system models – Part 2: Representation of water supply and allocation and opportunities for improved modeling. *Hydrology and Earth System Sciences*, 19, 63–90. https://doi.org/10.5194/hess-19-63-2015

Ngo, L. A., Masih, I., Jiang, Y., & Douven, W. (2018). Impact of reservoir operation and climate change on the hydrological regime of the Sesan and Srepok Rivers in the Lower Mekong Basin. *Climatic Change*, 149(1), 107–119. https://doi.org/10.1007/s10584-016-1875-y

Niu, G. Y., Yang, Z. L., Mitchell, K. E., Chen, F., Ek, M. B., Barlage, M., Kumar, A., Manning, K., Niyogi, D., Rosero, E., Tewari, M., & Xia, Y. (2011). The community Noah land surface model with multiparameterization options (Noah-MP): 1. Model description and evaluation with local-scale measurements. *Journal of Geophysical Research Atmospheres*, 116, 1–19. https://doi.org/10.1029/2010JD015139

Niu, Z., He, H., Zhu, G., Ren, X., Zhang, L., & Zhang, K. (2020). A spatial-temporal continuous dataset of the transpiration to evapotranspiration ratio in China from 1981–2015. *Scientific Data*, 7, 369. https://doi.org/10.1038/s41597-020-00693-x

Niyogi, D. S., Raman, S., Niyogi, D. S., & Raman, S. (1997). Comparison of four different stomatal resistance schemes using FIFE observations. *Journal of Applied Meteorology*, 36(7), 903–917. https://doi.org/10.1175/1520-0450(1997)036<0903:COFDSR>2.0.CO;2

Noilhan, J., & Planton, S. (1989). A simple parameterization of land surface processes for meteorological models. *Monthly Weather Review*, 117, 536–549. https://doi.org/10.1175/1520-0493(1989)117<0536:ASPOLS>2.0.CO;2

Oki, T., & Kanae, S. (2006). Global hydrological cycles and world water resources. *Science*, 313(5790), 1068–1072. https://doi.org/10.1126/science.1128845

Padiyedath Gopalan, S., Hanasaki, N., Champathong, A., & Tebakari, T. (2021). Impact assessment of reservoir operation in the context of climate change adaptation in the Chao Phraya River basin. *Hydrological Processes*, 35(1), 1–19. https://doi.org/10.1002/hyp.14005

Penman, H. L. (1948). Natural evaporation from open water, bare soil and grass. *Proceedings of the Royal Society of London. Series A. Mathematical and Physical Sciences*, 193(1032), 120–145.

Piao, S., Ciais, P., Huang, Y., Shen, Z., Peng, S., Li, J., Zhou, L., Liu, H., Ma, Y., Ding, Y., Friedlingstein, P., Liu, C., Tan, K., Yu, Y., Zhang, T., & Fang, J. (2010). The impacts of climate change on water resources and agriculture in China. *Nature*, 467(7311), 43–51. https://doi.org/10.1038/nature09364

Pitman, A. J. (2003). The evolution of, and revolution in, land surface schemes designed for climate models. *International Journal of Climatology*, 23(5), 479–510. https://doi.org/10.1002/joc.893

Pokhrel, Y. N., Hanasaki, N., Wada, Y., & Kim, H. (2016). Recent progresses in incorporating human land-water management into global land surface models toward their integration into Earth system models. *Wiley Interdisciplinary Reviews: Water*, 3(4), 548–574. https://doi.org/10.1002/wat2.1150

Powers, J. G., Klemp, J. B., Skamarock, W. C., Davis, C. A., Dudhia, J., Gill, D. O., Coen, J. L., Gochis, D. J., Ahmadov, R., Peckham, S. E., Grell, G. A., Michalakes, J., Trahan, S., Benjamin, S. G., Alexander, C. R., Dimego, G. J., Wang, W., Schwartz, C. S., Romine, G. S., ... Duda, M. G. (2017). The weather research and forecasting model: Overview, system efforts, and future directions. *Bulletin of the American Meteorological Society*, 98(8), 1717–1737. https://doi.org/10.1175/BAMS-D-15-00308.1

Priestley, C. H. B., & Taylor, R. J. (1972). On the assessment of surface heat flux and evaporation using large-scale parameters. *Monthly Weather Review*, *100*, 81–92. https://doi.org/10.1175/1520-0493 (1972)100<0081:otaosh>2.3.co;2

Prinn, R. G. (2013). Development and application of earth system models. *Proceedings of the National Academy of Sciences of the United States of America*, *110*, 3673–3680. https://doi.org/10.1073/pnas. 1107470109

Qian, Y., Huang, M., Yang, B., & Berg, L. K. (2013). A modeling study of irrigation effects on surface fluxes and land–air–cloud interactions in the southern Great Plains. *Journal of Hydrometeorology*, *14*, 700–721. https://doi.org/10.1175/JHM-D-12-0134.1

Rummler, T., Arnault, J., Gochis, D., & Kunstmann, H. (2019). Role of lateral terrestrial water flow on the regional water cycle in a complex terrain region: Investigation with a fully coupled model system. *Journal of Geophysical Research: Atmospheres*, *124*(2), 507–529. https://doi.org/10. 1029/2018JD029004

Sacks, W. J., Cook, B. I., Buenning, N., Levis, S., & Helkowski, J. H. (2009). Effects of global irrigation on the near-surface climate. *Climate Dynamics*, *33*, 159–175. https://doi.org/10.1007/s00382-008-0445-z

Savenije, H. H. G. (2004). The importance of interception and why we should delete the term evapotranspiration from our vocabulary. *Hydrological Processes*, *18*(8), 1507–1511. https://doi.org/10.1002/hyp. 5563

Schlesinger, W. H., & Jasechko, S. (2014). Transpiration in the global water cycle. *Agricultural and Forest Meteorology*, *189–190*, 115–117. https:// doi.org/10.1016/j.agrformet.2014.01.011

Senatore, A., Mendicino, G., Gochis, D. J., Yu, W., Yates, D. N., & Kunstmann, H. (2015). Fully coupled atmosphere-hydrology simulations for the central Mediterranean: Impact of enhanced hydrological parameterization for short and long time scales. *Journal of Advances in Modeling Earth Systems*, *7*(4), 1693–1715. https://doi.org/10.1002/ 2015MS000510

Shah, H. L., Zhou, T., Sun, N., Huang, M., & Mishra, V. (2019). Roles of irrigation and reservoir operations in modulating terrestrial water and energy budgets in the Indian Subcontinental River basins. *Journal of Geophysical Research: Atmospheres*, *124*(23), 12915–12936. https:// doi.org/10.1029/2019JD031059

Shankman, D., Keim, B. D., & Song, J. (2006). Flood frequency in China's Poyang lake region: Trends and teleconnections. *International Journal of Climatology*, *26*(9), 1255–1266. https://doi.org/10.1002/joc.1307

Sheffield, J., Wood, E. F., & Roderick, M. L. (2012). Little change in global drought over the past 60 years. *Nature*, *491*(7424), 435–438. https:// doi.org/10.1038/nature11575

Shin, S., Pokhrel, Y., & Miguez-Macho, G. (2019). High-resolution modeling of reservoir release and storage dynamics at the continental scale. *Water Resources Research*, *55*, 787–810. https://doi.org/10.1029/ 2018WR023025

Shrestha, P., Sulis, M., Masbou, M., Kollet, S., & Simmer, C. (2014). A scale-consistent terrestrial systems modeling platform based on COSMO, CLM, and ParFlow. *Monthly Weather Review*, *142*, 3466–3483. https://doi.org/10.1175/MWR-D-14-00029.1

Shrestha, P., Sulis, M., Simmer, C., & Kollet, S. (2015). Impacts of grid resolution on surface energy fluxes simulated with an integrated surface-groundwater flow model. *Hydrology and Earth System Sciences*, *19*(10), 4317–4326. https://doi.org/10.5194/hess-19-4317-2015

Shrestha, P., Sulis, M., Simmer, C., & Kollet, S. (2018). Effects of horizontal grid resolution on evapotranspiration partitioning using TerrSysMP. *Journal of Hydrology*, *557*, 910–915. https://doi.org/10.1016/j.jhydrol. 2018.01.024

Shuttleworth, W. J. (2012). *Terrestrial hydrometeorology*. Wiley-Blackwell. www.wiley.com/go/shuttleworth/hydrometeorology

Skamarock, W., Klemp, J., Dudhia, J., Gill, D., Barker, D., Wang, W., & Powers, J. G. (2008). *A description of the advanced research WRF version 3* (NCAR Technical Note NCAR/TN-475+STR). https://doi.org/10. 5065/D68S4MVH

Somers, L. D., Gordon, R. P., McKenzie, J. M., Lautz, L. K., Wigmore, O., Glose, A. M., Glas, R., Aubry-Wake, C., Mark, B., Baraer, M., & Condom, T. (2016). Quantifying groundwater–surface water interactions in a proglacial valley, Cordillera Blanca, Peru. *Hydrological Processes*, *30*, 2915–2929. https://doi.org/10.1002/hyp.10912

Sophocleous, M. (2002). Interactions between groundwater and surface water: The state of the science. *Hydrogeology Journal*, *10*, 52–67. https://doi.org/10.1007/s10040-001-0170-8

Sorooshian, S., Li, J., Hsu, K., & Gao, X. (2011). How significant is the impact of irrigation on the local hydroclimate in California's Central Valley? Comparison of model results with ground and remote-sensing data. *Journal of Geophysical Research*, *116*(D6), D06102. https://doi. org/10.1029/2010JD014775

Suen, J. P., & Eheart, J. W. (2006). Reservoir management to balance ecosystem and human needs: Incorporating the paradigm of the ecological flow regime. *Water Resources Research*, *42*, 1–9. https://doi.org/10. 1029/2005WR004314

Sun, S. L., Chen, H. S., Ju, W. M., Song, J., Li, J. J., Ren, Y. J., & Sun, J. (2012). Past and future changes of streamflow in Poyang Lake Basin, Southeastern China. *Hydrology and Earth System Sciences*, *16*, 2005–2020. https://doi.org/10.5194/hess-16-2005-2012

van der Ent, R. J., Wang-Erlandsson, L., Keys, P. W., & Savenije, H. H. G. (2014). Contrasting roles of interception and transpiration in the hydrological cycle – Part 2: Moisture recycling. *Earth System Dynamics*, *5*(2), 471–489. https://doi.org/10.5194/esd-5-471-2014

Veldkamp, T. I. E., Zhao, F., Ward, P. J., De Moel, H., Aerts, J. C. J. H., Schmied, H. M., Portmann, F. T., Masaki, Y., Pokhrel, Y., Liu, X., Satoh, Y., Gerten, D., Gosling, S. N., Zaherpour, J., & Wada, Y. (2018). Human impact parameterizations in global hydrological models improve estimates of monthly discharges and hydrological extremes: A multi-model validation study. *Environmental Research Letters*, *13*, 055008. https://doi.org/10.1088/1748-9326/aab96f

Wada, Y., Bierkens, M. F. P., De Roo, A., Dirmeyer, P. A., Famiglietti, J. S., Hanasaki, N., Konar, M., Liu, J., Schmied, H. M., Oki, T., Pokhrel, Y., Sivapalan, M., Troy, T. J., van Dijk, A. I. J. M., van Emmerik, T., Van Huijgevoort, M. H. J., Van Lanen, H. A. J., Vörösmarty, C. J., Wanders, N., & Wheater, H. (2017). Human-water interface in hydrological modelling: Current status and future directions. *Hydrology and Earth System Sciences*, *21*, 4169–4193. https://doi.org/10.5194/hess-21-4169-2017

Wada, Y., de Graaf, I. E. M., & van Beek, L. P. H. (2016). High-resolution modeling of human and climate impacts on global water resources. *Journal of Advances in Modeling Earth Systems*, *8*, 735–763. https://doi. org/10.1002/2015MS000618

Wagner, S., Fersch, B., Yuan, F., Yu, Z., & Kunstmann, H. (2016). Fully coupled atmospheric-hydrological modeling at regional and long-term scales: Development, application, and analysis of WRF-HMS. *Water Resources Research*, *52*(4), 3187–3211. https://doi.org/10.1002/ 2015WR018185

Wang, H., Guan, H., Liu, N., Soulsby, C., Tetzlaff, D., & Zhang, X. (2020). Improving the Jarvis-type model with modified temperature and radiation functions for sap flow simulations. *Journal of Hydrology*, *587*, 124981. https://doi.org/10.1016/j.jhydrol.2020.124981

Wang, L., Guo, S., Hong, X., Liu, D., & Xiong, L. (2017). Projected hydrologic regime changes in the Poyang Lake Basin due to climate change. *Frontiers of Earth Science*, *11*, 95–113. https://doi.org/10.1007/ s11707-016-0580-5

Wang, W., Lu, H., Ruby Leung, L., Li, H. Y., Zhao, J., Tian, F., Yang, K., & Sothea, K. (2017). Dam construction in Lancang-Mekong River basin could mitigate future flood risk from warming-induced intensified rainfall. *Geophysical Research Letters*, *44*, 10378–10386. https://doi.org/ 10.1002/2017GL075037

Wang-Erlandsson, L., van der Ent, R. J., Gordon, L. J., & Savenije, H. H. G. (2014). Contrasting roles of interception and transpiration in the hydrological cycle – Part 1: Temporal characteristics over land. *Earth System Dynamics*, 5(2), 441–469. https://doi.org/10.5194/esd-5-441-2014

Wei, J., Knoche, H. R., & Kunstmann, H. (2015). Contribution of transpiration and evaporation to precipitation: An ET-tagging study for the Poyang Lake region in Southeast China. *Journal of Geophysical Research: Atmospheres*, 120(14), 6845–6864. https://doi.org/10.1002/2014JD022975

Wei, J., Knoche, H. R., & Kunstmann, H. (2016). Atmospheric residence times from transpiration and evaporation to precipitation: An age-weighted regional evaporation tagging approach. *Journal of Geophysical Research: Atmospheres*, 121(12), 6841–6862. https://doi.org/10.1002/2015JD024650

Xie, Z., Liu, S., Zeng, Y., Gao, J., Qin, P., Jia, B., Xie, J., Liu, B., Li, R., Wang, Y., & Wang, L. (2018). A high-resolution land model with groundwater lateral flow, water use, and soil freeze-thaw front dynamics and its applications in an endorheic basin. *Journal of Geophysical Research: Atmospheres*, 123(14), 7204–7222. https://doi.org/10.1029/2018JD028369

Xu, X., Zhang, Q., Tan, Z., Li, Y., & Wang, X. (2015). Effects of water-table depth and soil moisture on plant biomass, diversity, and distribution at a seasonally flooded wetland of Poyang Lake, China. *Chinese Geographical Science*, 25, 739–756. https://doi.org/10.1007/s11769-015-0774-x

Yang, C., Lin, Z., Yu, Z., Hao, Z., & Liu, S. (2010). Analysis and simulation of human activity impact on streamflow in the Huaihe River basin with a large-scale hydrologic model. *Journal of Hydrometeorology*, 11, 810–821. https://doi.org/10.1175/2009JHM1145.1

Yao, Y., Tian, Y., Andrews, C., Li, X., Zheng, Y., & Zheng, C. (2018). Role of groundwater in the dryland ecohydrological system: A case study of the Heihe River basin. *Journal of Geophysical Research: Atmospheres*, 123(13), 6760–6776. https://doi.org/10.1029/2018JD028432

Ye, X., Zhang, Q., Liu, J., Li, X., & Xu, C. (2013). Distinguishing the relative impacts of climate change and human activities on variation of streamflow in the Poyang Lake catchment, China. *Journal of Hydrology*, 494, 83–95. https://doi.org/10.1016/j.jhydrol.2013.04.036

Yigzaw, W., Li, H. Y., Fang, X., Leung, L. R., Voisin, N., Hejazi, M. I., & Demissie, Y. (2019). A multilayer reservoir thermal stratification module for earth system models. *Journal of Advances in Modeling Earth Systems*, 11, 3265–3283. https://doi.org/10.1029/2019MS001632

Yu, Z. (2000). Assessing the response of subgrid hydrologic processes to atmospheric forcing with a hydrologic model system. *Global and Planetary Change*, 25, 1–17. https://doi.org/10.1016/S0921-8181(00)00018-7

Yu, Z., Pollard, D., & Cheng, L. (2006). On continental-scale hydrologic simulations with a coupled hydrologic model. *Journal of Hydrology*, 331(1–2), 110–124. https://doi.org/10.1016/j.jhydrol.2006.05.021

Yu, Z., & Schwartz, F. W. (1998). Application of an integrated basin-scale hydrologic model to simulate surface-water and ground-water interactions. *Journal of the American Water Resources Association*, 34(2), 409–425. https://doi.org/10.1111/j.1752-1688.1998.tb04145.x

Yuan, F., Kunstmann, H., Yang, C., Yu, Z., Ren, L., Fersch, B., & Xie, Z. (2009). *Development of a coupled land-surface and hydrology model system for mesoscale hydrometeorological simulations* (pp. 195–202). IAHS Publication. http://cat.inist.fr/?aModele=afficheN&cpsidt=22437463

Yue, T., Nixdorf, E., Zhou, C., Xu, B., Zhao, N., Fan, Z., Huang, X., Chen, C., & Kolditz, O. (Eds.). (2019). *Chinese water systems*. Springer International Publishing. https://doi.org/10.1007/978-3-319-97725-6

Zajac, Z., Revilla-Romero, B., Salamon, P., Burek, P., Hirpa, F., & Beck, H. (2017). The impact of lake and reservoir parameterization on global streamflow simulation. *Journal of Hydrology*, 548, 552–568. https://doi.org/10.1016/j.jhydrol.2017.03.022

Zeng, X., & Decker, M. (2009). Improving the numerical solution of soil moisture-based Richards equation for land models with a deep or shallow water table. *Journal of Hydrometeorology*, 10(1), 308–319. https://doi.org/10.1175/2008JHM1011.1

Zhang, Q., Sun, P., Jiang, T., Tu, X., & Chen, X. (2011). Spatio-temporal patterns of hydrological processes and their responses to human activities in the Poyang Lake basin, China. *Hydrological Sciences Journal*, 56, 305–318. https://doi.org/10.1080/02626667.2011.553615

Zhang, Q., Xiao, M., Singh, V. P., & Wang, Y. (2016). Spatiotemporal variations of temperature and precipitation extremes in the Poyang Lake basin, China. *Theoretical and Applied Climatology*, 124(3–4), 855–864. https://doi.org/10.1007/s00704-015-1470-6

Zhang, X., Xiao, Y., Wan, H., Deng, Z., Pan, G., & Xia, J. (2017). Using stable hydrogen and oxygen isotopes to study water movement in soil-plant-atmosphere continuum at Poyang Lake wetland, China. *Wetlands Ecology and Management*, 25, 221–234. https://doi.org/10.1007/s11273-016-9511-1

Zhang, Z., Arnault, J., Wagner, S., Laux, P., & Kunstmann, H. (2019). Impact of lateral terrestrial water flow on land-atmosphere interactions in the Heihe River Basin in China: Fully coupled modeling and precipitation recycling analysis. *Journal of Geophysical Research: Atmospheres*, 124, 8401–8423. https://doi.org/10.1029/2018JD030174

Zhao, G., Gao, H., Naz, B. S., Kao, S. C., & Voisin, N. (2016). Integrating a reservoir regulation scheme into a spatially distributed hydrological model. *Advances in Water Resources*, 98, 16–31. https://doi.org/10.1016/j.advwatres.2016.10.014

Zhao, Y., Dong, N., & Wang, H. (2021). Quantifying the climate and human impacts on the hydrology of the Yalong River basin using two approaches. *River Research and Applications*, 37, 591–604. https://doi.org/10.1002/rra.3782

Zheng, H., Yang, Z. L., Lin, P., Wei, J., Wu, W. Y., Li, L., Zhao, L., & Wang, S. (2019). On the sensitivity of the precipitation partitioning into evapotranspiration and runoff in land surface parameterizations. *Water Resources Research*, 55, 95–111. https://doi.org/10.1029/2017WR022236

Zhou, H., Zhou, W., Liu, Y., Yuan, Y., Huang, J., & Liu, Y. (2020). Meteorological drought migration in the Poyang Lake Basin, China: Switching among different climate modes. *Journal of Hydrometeorology*, 21(3), 415–431. https://doi.org/10.1175/JHM-D-19-0183.1

Zhou, T., Nijssen, B., Gao, H., & Lettenmaier, D. P. (2016). The contribution of reservoirs to global land surface water storage variations. *Journal of Hydrometeorology*, 17, 309–325. https://doi.org/10.1175/JHM-D-15-0002.1

Zou, J., Xie, Z., Zhan, C., Qin, P., Sun, Q., Jia, B., & Xia, J. (2015). Effects of anthropogenic groundwater exploitation on land surface processes: A case study of the Haihe River basin, northern China. *Journal of Hydrology*, 524, 625–641. https://doi.org/10.1016/j.jhydrol.2015.03.026

SUPPORTING INFORMATION